Deep-Sea Research II 56 (2009) 1502–1518

Contents lists available at ScienceDirect

Deep-Sea Research II

journal homepage: www.elsevier.com/locate/dsr2

POC export from ocean surface waters by means of $^{234}Th/^{238}U$ and $^{210}Po/^{210}Pb$ disequilibria: A review of the use of two radiotracer pairs

Elisabet Verdeny [a,*], Pere Masqué [a,b], Jordi Garcia-Orellana [a,b], Claudia Hanfland [c], J. Kirk Cochran [d], Gillian M. Stewart [e]

[a] Departament de Física, Universitat Autònoma de Barcelona, 08193 Bellaterra, Spain
[b] Institut de Ciència i Tecnologia Ambientals, Universitat Autònoma de Barcelona, 08193 Bellaterra, Spain
[c] Marine Geochemistry, Alfred Wegner Institute for Polar and Marine Research, 27570 Bremerhaven, Germany
[d] Marine Sciences Research Center, Stony Brook University, Stony Brook, NY 11794, USA
[e] School of Earth and Environmental Sciences, Queens College, NY 11367, USA

ARTICLE INFO

Available online 25 December 2008

Keywords:
Carbon flux
POC
Export production
Thorium
Polonium

ABSTRACT

^{234}Th ($T_{1/2}$ = 24.1 d) and ^{210}Po ($T_{1/2}$ = 138.4 d) are particle reactive radioisotopes that are used as tracers for particle cycling in the upper ocean. Particulate organic carbon (POC) export has frequently been estimated using $^{234}Th/^{238}U$ disequilibrium. Recent evidence suggests that $^{210}Po/^{210}Pb$ disequilibrium may be used as an additional tool to examine particle export, given the direct biological uptake of ^{210}Po into cellular material. Differences in these two radioisotope pairs with regard to their half-lives, particle reactivity and scavenging affinity in seawater should provide complementary information to be obtained on the processes occurring in the water column. Here, we review eight different studies that have simultaneously used both approaches to estimate POC export fluxes from the surface ocean. Our aim is to provide a complete "dataset" of all the existing POC flux data derived from the coupled use of both ^{234}Th and ^{210}Po and to evaluate the advantages and limitations of each tracer pair. Our analysis suggests that the simultaneous use of both radiotracers provides more useful comparative data than can be derived from the use of a single tracer alone. The difference in half-lives of ^{234}Th and ^{210}Po enables the study of export production rates over different time scales. In addition, their different biogeochemical behaviour and preferred affinity for specific types of particles leads to the conclusion that ^{234}Th is a better tracer of total mass flux, whereas ^{210}Po tracks POC export more specifically. The synthesis presented here is also intended to provide a basis for planning future sampling strategies and promoting further work in this field to help reveal the more specific application of each tracer under specific water column biogeochemistries.

1. Introduction

Understanding the natural mechanisms of oceanic carbon dioxide (CO_2) uptake is essential for the reliable forecast of future changes in atmospheric CO_2, nowadays very much related to the increased anthropogenic emissions of greenhouse gases to the atmosphere. One such mechanism is the "biological pump", the conversion of CO_2 into biomass. Most of the CO_2 taken up by phytoplankton is recycled near the surface, but a variable and significant amount of the biomass carbon leaves the euphotic zone and sinks into the deep waters via gravitational settling, diffusion and active biotransport of organic carbon and inorganic carbon (i.e. $CaCO_3$) (Ducklow et al., 2001). As this material, often called marine snow, sinks through the water column a large proportion of this biomass is converted back to CO_2 by marine bacteria, and less than 1% ultimately reaches the seafloor (Feely et al., 2001; Berelson et al., 2002). The efficiency of the biological pump can therefore be expressed as the ratio of the amount of particulate carbon exported from the surface layer relative to the total amount produced through photosynthesis (Eppley and Peterson, 1979; Ducklow et al., 2001).

In this study, we examine the use of ^{234}Th and ^{210}Po as tracers of export production from the upper ocean and, more specifically, of particulate organic carbon (POC) flux. A total of eight different studies that include simultaneous measurements of both ^{238}U–^{234}Th and ^{210}Pb–^{210}Po disequilibria to estimate POC export fluxes are reviewed. These studies were undertaken in various regions of the world's ocean: Southern Ocean, South and mid-Atlantic Ocean, Sargasso Sea, Mediterranean Sea and Equatorial Pacific (see Fig. 1). By compiling a complete "dataset" of all the

* Corresponding author. Tel.: +34 93 581 1191; fax: +34 93 581 2155.
E-mail address: elisabet.verdeny@uab.cat (E. Verdeny).

0967-0645/$ - see front matter © 2009 Published by Elsevier Ltd.
doi:10.1016/j.dsr2.2008.12.018

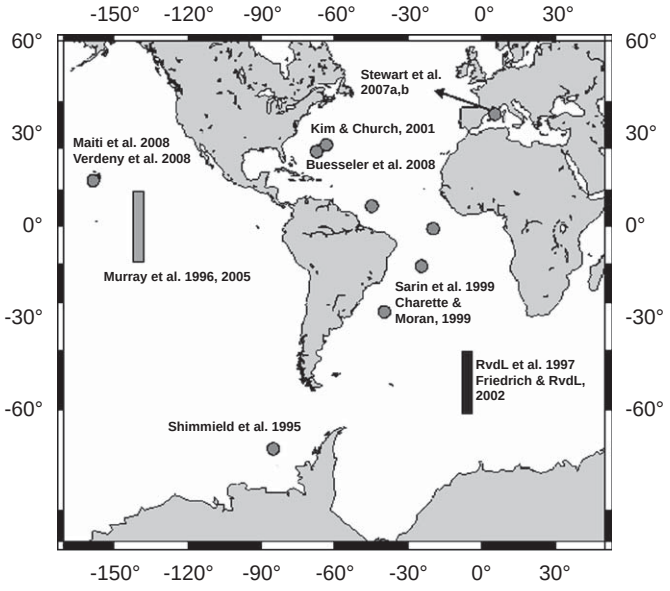

Fig. 1. Location of study sites under review. The dots represent sampling stations or sampling areas, and the bars represent sampling transects along a given meridian.

existing POC fluxes derived from the coupled use of both tracers, our goal is to evaluate the advantages and disadvantages, as well as possible limitations, of the use of ^{234}Th and ^{210}Po as tracers of POC export production. We will discuss whether the simultaneous application of both approaches can provide more information than can be derived from the use of either tracer alone.

1.1. Measurements of POC export

1.1.1. Sediment traps

Sediment traps are widely used to measure the vertical flux of particulate matter in the oceans: they provide insights into the spatial and temporal variability of fluxes and composition of sinking particles, and have come to be one of the principal methods for understanding the marine carbon cycle (i.e. Honjo et al., 1982, 1995, 2000). Sediment traps have been used to determine the extent to which CO_2 fixed by primary producers is exported as POC. Data collected in sediment traps indicate that the POC flux decreases: (1) with increasing depth; (2) with increasing distance from the continental margin; and (3) with decreasing primary production (Martin et al., 1987; Armstrong et al., 2001). However, three major factors have been identified as potentially biasing the results obtained using sediment traps, at least in terms of quantitative flux measurements: zooplankton swimmers (Lee et al., 1988; Karl and Knauer, 1989; Michaels et al., 1990), particle solubilization (Knauer et al., 1990) and hydrodynamics (Gardner, 1980; Gust et al., 1992, 1994) (see a review by Buesseler et al., 2007).

1.1.2. Use of radioactive tracers

Indirect estimates of particle fluxes can be attained from the use of particle reactive radiotracers. Since radionuclides are produced and decay at known rates, they are useful for quantifying time-dependent processes. If these radionuclides are also particle reactive they will tend to be absorbed, and/or adsorbed, onto particles and track their progress through the water column. Therefore, a combination of these two characteristics is required for these tracers to become a potential tool for quantifying particulate export fluxes. The export flux of a given parameter (i.e. POC) can be estimated if the ratio of the concentration of the parameter to the radionuclide in sinking particles is known. For the study of upper ocean processes, the short-lived particle reactive isotopes of the ^{238}U decay series, ^{234}Th ($T_{1/2}=24.1$ d) and ^{210}Po ($T_{1/2}=138.4$ d), are particularly suitable tracers because of their half-lives and scavenging affinity (Coale and Bruland, 1985; Bacon et al., 1976, 1988).

1.1.2.1. ^{234}Th/^{238}U disequilibrium. The disequilibrium between ^{234}Th and its parent ^{238}U has most often been used to estimate the flux of POC (Buesseler et al., 1992; Cochran et al., 1995; Bacon et al., 1996; Moran et al., 1997; Benitez-Nelson et al., 2001; Benitez-Nelson and Moore, 2006). ^{234}Th is produced continuously in seawater through alpha decay of its soluble parent nuclide ^{238}U (half-life $=4.5\times10^9$ yr) and is very particle reactive (Bacon and Anderson, 1982; Moore and Hunter, 1985). Uranium is conservative in seawater at a concentration of approximately 3.1 μg L^{-1} because it remains dissolved as the $UO_2(CO_3)_3^{4-}$ species (Langmuir, 1978; Chen et al., 1986; Pates and Muir, 2007). Dissolved thorium exists as the hydrolysis product $Th(OH)_n^{(4-n)+}$ but is quickly removed from the dissolved state by adsorption onto particles (Honeyman et al., 1988; Santschi et al., 2006). In the absence of Th scavenging and export by particles, we would expect to find ^{238}U and ^{234}Th in secular equilibrium, both with a concentration of approximately 2.4–2.6 dpm L^{-1}. But because the ocean is not particle free, thorium is effectively scavenged onto particle surfaces and removed from the surface ocean as these particles sink, creating a deficiency of ^{234}Th relative to ^{238}U, of 0.8 typically. An idealized oceanic profile shows relatively low dissolved ^{234}Th activity in the surface waters, where scavenging is more intense, and an increase in ^{234}Th activity with depth as particle concentration decreases; a return to secular equilibrium usually occurs at depths of 50–200 m.

The half-life of ^{234}Th (24.1 d) is very suitable for tracing events occurring over short time scales of days to weeks, similar to the development of a phytoplankton bloom and the subsequent related particle export. The ^{234}Th deficiency relative to ^{238}U is thus used to calculate the removal flux of ^{234}Th through scavenging on sinking particles (see Cochran and Masqué (2003) for a review and references therein). The removal of ^{234}Th can then be used to estimate the POC flux if the POC/^{234}Th ratio in settling particles is ascertained (e.g. Buesseler et al., 2006).

1.1.2.2. ^{210}Po/^{210}Pb disequilibrium. ^{226}Ra ($T_{1/2}=1600$ yr) is produced from ^{230}Th in the ^{238}U decay chain and decays to ^{222}Rn ($T_{1/2}=3.8$ d) through alpha decay. A fraction of ^{222}Rn continuously escapes from soils and, once in the atmosphere, decays through a series of short half-life products to ^{210}Pb ($T_{1/2}=22.3$ yr), which is particle reactive and associates with aerosols (Turekian et al., 1977). The residence time of ^{210}Pb in the atmosphere is on the order of days to weeks and it is deposited onto land and ocean surface by both dry and wet deposition (Moore et al., 1974; Turekian et al., 1977; Kritz, 1983). In marine systems, water column ^{210}Pb is also produced by *in situ* decay of ^{226}Ra, which has nutrient like distributions in seawater (Broecker et al., 1967; Ku et al., 1970; Ku and Lin, 1976). *In situ* production of ^{210}Pb in the shallow waters of coastal areas is almost negligible compared to the atmospheric flux. In contrast, *in situ* production of ^{210}Pb represents a much greater contribution in the open ocean, although excess ^{210}Pb relative to ^{226}Ra may also be significant due to atmospheric input (Cochran, 1992). ^{210}Po is produced by decay of ^{210}Pb via its short-lived daughter, ^{214}Bi. Due to the short residence time of ^{210}Pb in the atmosphere, ^{210}Po concentrations in aerosols, and thus fluxes to the surface ocean waters, are only about 10–20% that of ^{210}Pb (Lambert et al., 1982). Therefore, the main source of ^{210}Po in seawater is the *in situ* decay of ^{210}Pb, which presents typical

activities varying between 10 and 20 dpm $100\,L^{-1}$, depending on the region.

The half-life of ^{210}Po ($T_{1/2} = 128.4$ d) is much shorter than that of ^{210}Pb, and, like ^{234}Th and ^{238}U, they would be in secular equilibrium in the ocean in the absence of sinking particles. However, a deficiency of ^{210}Po relative to ^{210}Pb is often observed through the upper few hundred metres of the water column, leading to a typical ^{210}Po/^{210}Pb total activity ratio in the surface ocean of about 0.5 (Bacon et al., 1976; Nozaki et al., 1976; Cochran, 1992). The disequilibrium is primarily due to a difference in Po and Pb biogeochemistry. Pb and Po are both particle reactive although they have different chemical behaviours: Po has a stronger affinity for particles than Pb (Kharkar et al., 1976; Heyraud et al., 1976). Pb and Po also have different binding mechanisms: while Pb is only adsorbed onto particle surfaces (it behaves similarly to Th), Po is also assimilated into phytoplankton cells, by entering the biological cycle of the living organisms in a manner similar to sulphur. Thus, Po becomes enriched in organic soft tissue, specifically proteins, and can bioaccumulate within the food web (Fisher et al., 1983; Cherrier et al., 1995; Stewart and Fisher, 2003a, b; Stewart et al., 2005). Common values of the ^{210}Po/^{210}Pb ratio are 3 for phytoplankton and 12 for zooplankton (Shannon et al., 1970; Turekian et al., 1974; Kharkar et al., 1976) suggesting that ^{210}Po is enriched within the food web.

As pointed out in seminal works by Turekian et al. (1974), Nozaki and Turekian (1976) and Bacon et al. (1976) the ^{210}Pb–^{210}Po pair can be used to trace particle transport processes and quantify chemical scavenging and particle removal rates in the upper ocean for time scales of weeks to months. Recent experimental studies by Stewart and Fisher (2003a, b) and Stewart et al. (2007a, b) give further support to the use of ^{210}Po as a tracer for organic matter in the ocean.

However, only a few studies have applied the ^{210}Po/^{210}Pb disequilibrium to estimate the POC export flux in a fashion similar to the ^{234}Th/^{238}U pair. Here we review five different studies from the literature where both approaches have been used. In some instances, however, the original studies did not apply the two approaches in an identical manner and we have re-examined the data for use in this work. We also include results from a recent study conducted within the framework of the MedFlux programme in the Mediterranean Sea (Stewart et al., 2007a, b), as well as results from two other projects, EDDIES (Buesseler et al., 2008) and E-Flux (Maiti et al., 2008; Verdeny et al., 2008) that have studied the export production within mesoscale eddies in the Sargasso Sea and in the North Tropical Pacific near Hawaii, respectively.

1.2. Calculation methodology and POC flux determination

The studies summarized here had significant differences in the manner in which water column radionuclide fluxes were calculated and then translated into POC fluxes. In order to present a unified dataset of radionuclide and POC fluxes, we must first use a consistent methodology. We therefore re-calculated the inventories and the integrated deficiencies of ^{234}Th and ^{210}Po using the following approach. The water column was divided into boxes spanning the distance between two consecutive mid points (z) placed at the mean distance between two consecutive sampling depths:

$$z = z_i + \frac{z_{i+1} - z_i}{2} \tag{1}$$

The width (w_i) of the boxes is calculated by

$$w_i = \left(z_i + \frac{z_{i+1} - z_i}{2}\right) - \left(z_{i-1} + \frac{zi - z_{i-1}}{2}\right) \tag{2}$$

and the integrated inventory (I, in dpm m^{-2}) of ^{234}Th and ^{210}Po is obtained using a simple box integration model:

$$I = A_1 w_1 + A_2 w_2 + A_3 w_3 + \cdots \tag{3}$$

where A_i is the activity of ^{234}Th or ^{210}Po determined at any given sampling depth i.

The fluxes of ^{234}Th and ^{210}Po were calculated using a two-box irreversible scavenging model (Bacon et al., 1976). When only total activities of the radionuclide were available, we applied a one-box irreversible model (Matsumoto, 1975). If A_1 and A_2 are the parent and daughter activities, respectively, the change of total A_2 activity with time is given by

$$\frac{dA_2^t}{dt} = [\phi(A_2)] + A_1^t \lambda_2 - A_2^t \lambda_2 - P_2 + V_t \tag{4}$$

or, considering dissolved (d) and particulate (p) fractions separately by

$$\frac{dA_2^d}{dt} = [\phi_d(A_2)] + A_1^d \lambda_2 - A_2^d \lambda_2 - J_2 + V_d \tag{5}$$

$$\frac{dA_2^p}{dt} = [\phi_p(A_2)] + J_2 + A_1^p \lambda_2 - A_2^p \lambda_2 - P_2 + V_p \tag{6}$$

where A^t, A^d and A^p are the total, dissolved and particulate activities, respectively, J_2 and P_2 are the scavenging and removal fluxes of the daughter nuclides, respectively, V the "physics" term and accounts for processes such as upwelling and diffusion, λ the radioactive decay constant for each radionuclide, and Φ the atmospheric flux (only appropriate for the ^{210}Po–^{210}Pb pair). If the atmospheric deposition of ^{210}Po is considered negligible and physical processes are ignored, the removal flux (P) of ^{234}Th or ^{210}Po between two different depths, z_1 and z_2, can be calculated, for steady state (SS) and non-steady state (NSS), respectively, from

$$P_2 = \int_{z_1}^{z_2} (A_1^T - A_2^T)\lambda_2 \, dz \tag{7}$$

$$P_2 = \lambda_2 \left[\frac{A_2(1 - e^{-\lambda_2 \Delta t}) + A_{2_{t1}}^T e^{-\lambda_2 \Delta t} - A_{2_{t2}}^T}{1 - e^{-\lambda_2 \Delta t}}\right] \tag{8}$$

In one case study (the Equatorial Pacific), a physical advection term was included (see Section 2.5). When data were available, a non-steady state approach was used (see Sections 2.3 and 2.4).

POC fluxes were re-calculated using a variety of methods depending on the availability of the particulate carbon data. When possible we have used the POC/radionuclide ratio measured in particles from sediment traps at the base of the euphotic zone, and/or the ratio determined in the large particles from *in situ* pump samples (>53 or 70 μm), and/or the ratio on suspended particles (typically >1 μm). Alternatively, we used the inventory of POC in the water column and the residence times of particulate ^{234}Th and ^{210}Po in the upper water column. In some cases we found slightly different results with respect to the fluxes calculated by the authors, which we attribute to the different way we integrated the water column deficiencies. For consistency, we have used our re-calculated results, which also provided ^{210}Po-POC flux estimates for some studies where they were not originally determined (Atlantic Ocean, Sargasso Sea and Equatorial Pacific).

2. Case studies

The studies presented in this work are the only published studies in which vertical activity profiles of ^{234}Th, ^{210}Pb and ^{210}Po were sampled at the same sites and times, and ^{234}Th/^{238}U and ^{210}Po/^{210}Pb disequilibria were calculated to estimate POC export.

Table 1
Summary of sampling techniques for all case studies under review.

Case study	Th	Po, Pb	POC	POC/Th	POC/Po
Bellingshausen Sea, Antarctica Shimmield et al. (1995)	*In situ* pump GFF 1 μm	23 L 0.45 μm	*In situ* pump GFF 1 μm	>1 μm *In situ* pump	nd[a]
Atlantic Ocean Sarin et al. (1999) Charette and Moran (1999)	*In situ* pump 53 and 0.7 μm	20 L 0.7 μm GFF	*In situ* pump 53 and 0.7 μm	*In situ* pump >53 μm	nd[a]
Antarctic Circumpolar current Rutgers van der Loeff et al. (1997) Friedrich and Rutgers van der Loeff (2002)	50–250 L 1 μm	50–250 L 1 μm	Small volume 0.7 μm GFF	Niskin Bottles >1 μm	Niskin Bottles >1 μm
Sargasso Sea Kim and Church (2001)	20 L 0.45 μm	20 L 0.45 μm	Small volume 0.7 μm GFF	nd[a,b]	nd[a,b]
Central Equatorial Pacific Murray et al. (1996, 2005)	20 L 0.45/0.50 μm	20 L 0.45/0.50 μm	4–6 L GFF 1 μm	Sediment trap	Sediment trap
Mediterranean Sea (MedFlux) Stewart et al. (2007a, b)	*In situ* pump 70 and 1 μm filters	Small volume 10 L 0.2 μm filtered	*In situ* pump 70 and 1 μm filters	Sed. trap and *in situ* pump >70 μm	Sed. trap and *in situ* pump >70 μm
Sargasso Sea (EDDIES) Buesseler et al. (2008)	Small volume 4 L Total activities	Small volume 8–10 L Total activities	nd[a]	Sed. trap and *in situ* pump >53 μm	*In situ* pump >53 μm
North Tropical Pacific, Hawaii (EFlux) Maiti et al. (2008) Verdeny et al. (2008)	Small volume 4 L Total activities	Small volume 8–10 L Total activities	*In situ* pump 53 μm and sediment trap	*In situ* pump > 53 μm and sediment trap	nd[a]

[a] Not determined.
[b] No primary data available to calculate the ratios.

Table 2
Published and re-calculated POC flux results for the study in the Bellingshausen Sea, Antarctica (Shimmield et al., 1995).

Station	Depth (m)	POC/^{234}Th (μmol dpm^{-1})	Inv. POC (mmol m^{-2})	^{234}Th–POC flux (mmol m^{-2} d^{-1})	^{210}Po–POC flux (mmol m^{-2} d^{-1})
Published results (SS)					
Sta. K	0–100	13.5[a]	727	21	2.2
Re-calculated results (SS)					
Sta. K	0–100	13.5[a]	727	24±5	2.3±0.5
		6.5[b]		17.2±3.3 8.3±1.6	

[a] Integrated value of the POC/^{234}Th ratio at the 0–100 m section (>1 μm).
[b] Value of the POC/^{234}Th ratio at the base of the mixed layer, at 100 m (>1 μm).

For each study, we briefly summarize the sampling scheme and methodologies (see Table 1 for the compilation of the sampling methods). For each case under review, we include a section that discusses and presents the approach/es used for re-calculating the POC flux in order to obtain better comparative estimates, always limited by the availability of C data. We note that for the three most recent studies (in Sections 2.6, 2.7 and 2.8) the ^{234}Th and ^{210}Po fluxes were originally determined as in Eqs. (1)–(7), and the ^{234}Th–POC and ^{210}Po–POC fluxes were obtained with comparisons. The POC flux results are compiled in Tables 2–9 and plotted in Figs. 2A–H.

2.1. Bellingshausen Sea, Antarctica (Shimmield et al., 1995)

Vertical distributions of dissolved and particulate ^{210}Pb, ^{210}Po and ^{234}Th were measured at one site (Station K) in the Bellingshausen Sea. We re-calculated the ^{234}Th–POC flux using the ^{234}Th deficiency and the value of the POC/^{234}Th ratio in large volume particulate (on GFF) samples from the base of the euphotic zone (100 m). The ^{210}Po-derived POC fluxes were re-calculated using the inventory of POC in the upper 100 m and the residence time of particulate ^{210}Po (>45 μm). For comparative purposes, we have also obtained the ^{234}Th–POC fluxes using the

Table 3
Published and re-calculated POC flux results for the study in the Atlantic Ocean (Charette and Moran, 1999; Sarin et al., 1999).

Station	Depth (m)	POC/^{234}Th (μmol dpm^{-1})	POC/^{210}Po (μmol dpm^{-1})	^{234}Th–POC flux (mmol m^{-2} d^{-1})	^{210}Po–POC flux (mmol m^{-2} d^{-1})
Published results (SS)					
Sta. 10	0–110	Not specified in the paper	Not specified in the paper	12	Not calculated by the authors
Sta. 8	0–150			4.6	
Sta. RFZ	0–100			0	
Sta. 6	0–150			8	
Re-calculated results (SS)					
Sta. 10	0–110	3.8±0.3[b]	56±12[b]	1.5±0.8	2.8±0.7
Sta. 8	0–150	2.8±0.3[b]	233±329[b]	3.5±2.4	7±10
Sta. RFZ	0–100	2.7±0.3[b]	59±36[b]	1.1±0.6	1.4±0.9
Sta. 6	0–150	2.5±0.3[b]	105±85[b]	3.8±2.0	8.5±6.9
Sta. 10	0–110	42±10[a]		16.8±9.9	
Sta. 8	0–150	3.9±0.5[a]		4.9±3.3	
Sta. RFZ	0–100	19.9±1.3[a]		7.8±4.4	
Sta. 6	0–150	8.0±0.8 [a]		12.2±6.4	

[a] POC/^{234}Th ratio measured in > 53 μm particles from *in situ* pumps.
[b] POC/^{234}Th(^{210}Po) ratio measured in >0.7 μm particles from *in situ* pumps.

Table 4
Published and re-calculated POC flux results for the study in the Antarctic circumpolar current (Rutgers van der Loeff et al., 1997; Friedrich and Rutgers van der Loeff, 2002). Location of the eight stations considered under study. SACC = South Antarctic Circumpolar Current; MIZ = Marginal Ice Zone; PFr = Polar Front region.

Latitude	Stations in transect			Depth (m)	^{234}Th–POC flux[a] (mmol m^{-2} d^{-1})		^{210}Po–POC flux[a] (mmol m^{-2} d^{-1})	
	2	5	11		2–5	5–11	2–5	5–11
Published results (NSS)								
SACC 57°S			941					
MIZ 53°S			949					
MIZ 51°S		899	953	0–100		11–20		17.4
PFr 49°S	877[b]	903	960	0–100	9–22	11–21		14.1
PFr 47–48°S	879	907						
Re-calculated results (NSS)								
51°S		899	953	0–100		63±11		16±12
49°S	877[b]	903	960	0–100	22±6	25±1	49±10	5±9

Re-calculated results (SS)

Station	Depth (m)	POC/^{234}Th[a] (μmol dpm^{-1})	POC/^{210}Po[a] (μmol dpm^{-1})	^{234}Th–POC flux (mmol m^{-2} d^{-1})	^{210}Po–POC flux (mmol m^{-2} d^{-1})
879	0–60	19.1±0.4	673±36	5.7±1.6	4.8±0.9
899	0–100	44.9±1.8	1100±128	21.6±5.7	16.2±2.5
903	0–100	17.6±0.4	664±42	10.5±1.8	7.5±0.9
907	0–100	22.7±0.8	965±91	3.9±2.4	14.6±1.8
941	0–100	38.0±1.7	361±17	9.1±5.1	7.3±0.6
949	0–100	40.4±1.8	387±17	28.3±5.2	6.7±0.5
953	0–100	37.1±1.3	1205±82	38.4±4.4	17.1±1.7
960	0–100	14.0±0.3	880±42	15.9±1.3	12.5±1.3

[a] Ratio determined from > 0.7 μm 1–2 L samples (POC) and >1 μm particles from Niskin samples (^{234}Th and ^{210}Po).
[b] Station taken as reference for the NSS calculations. Primary POC data was missing for this station.

inventory of the POC in the upper 100 m and the residence time of particulate ^{234}Th. These additional calculations will be used to discuss the results (Table 2).

2.2. Atlantic Ocean (Charette and Moran, 1999; Sarin et al., 1999)

Seawater samples were taken at four stations along a transect through the mid-Atlantic, from 35°S to 10°N during May and June of 1996. This transect included two stations in the South Atlantic (33°S 40°W; 17°S 25°W) and two in the equatorial Atlantic (0.5°S 20°W; 8°N 45°W), allowing a comparison between the particle-associated scavenging processes in the equatorial and subtropical regions of the South Atlantic. The distributions of ^{210}Po and ^{210}Pb were measured in the dissolved (<0.7 μm) and total (dissolved+particulate) phases of seawater samples in the upper 500 m. ^{234}Th was also measured in the upper 500 m at the same stations in the dissolved, particulate (0.7–53 μm and >53 μm) and total fractions. POC was measured in both particle size classes (0.7–53 and >53 μm).

For the ^{210}Po/^{210}Pb disequilibrium, Sarin et al. (1999) plotted the ^{210}Po deficiency against POC data (measured in the >0.7 μm

Table 5
Published and re-calculated POC flux results for the study in the Sargasso Sea (BATS station) (Kim and Church, 2001).

Station	Depth (m)	Inv. POC ($mmol\,m^{-2}$)	ST POC flux ($mmol\,m^{-2}\,d^{-1}$)	^{234}Th–POC flux ($mmol\,m^{-2}\,d^{-1}$)	^{210}Po–POC flux ($mmol\,m^{-2}\,d^{-1}$)
Published results (SS)					
Oct.	0–150	271	2.9	19	Not calculated by the authors
Dec.	0–150	358	5.6	66	
Feb.	0–150	269	2.6	10	
Apr.	0–150	409	2.2	2	
Jun.	0–150	341	1.9	33	
Aug.	0–150	338	3.5	18	
Re-calculated results (SS)					
Oct.	0–150	271	2.9	8.8 ± 0.0	6.7 ± 0.6
Dec.	0–150	358	5.6	24.5 ± 0.0	8.0 ± 0.6
Feb.	0–150	269	2.6	5.7 ± 0.2	5.1 ± 0.3
Apr.	0–150	409	2.2	0.3 ± 69.9	2.7 ± 0.1
Jun.	0–150	341	1.9	10.7 ± 0.0	2.4 ± 0.1
Aug.	0–150	338	3.5	5.9 ± 0.0	2.9 ± 0.1
Re-calculated results (NSS)					
Oct.	0–150	271	2.9		
Dec.	0–150	358	5.6	24.9 ± 9.2	9.1 ± 0.8
Feb.	0–150	269	2.6	3.4 ± 2.4	3.8 ± 0.3
Apr.	0–150	409	2.2	-1.1 ± 3.1	-0.3 ± 0.2
Jun.	0–150	341	1.9	11.8 ± 1.7	3.4 ± 0.2
Aug.	0–150	338	3.5	5.0 ± 1.3	2.7 ± 0.2

Table 6
Published and re-calculated POC flux results for the study in the Central Equatorial Pacific (Murray et al., 1996, 2005; Survey I).

Station	Depth (m)	POC/^{234}Th[a] ($\mu mol\,dpm^{-1}$)	POC/^{210}Po[a] ($\mu mol\,dpm^{-1}$)	ST POC flux ($mmol\,m^{-2}\,d^{-1}$)	^{234}Th–POC flux[b] ($mmol\,m^{-2}\,d^{-1}$)		^{210}Po–POC flux[b] ($mmol\,m^{-2}\,d^{-1}$)	
Published results (SS)								
St. 1	0–120	Values in graphs in	Values in graphs in	4.8	1.7			
St. 2	0–120	Murray et al. (1996)	Murray et al. (2005)	4.3	3.2			
St. 3	0–120			5.3	2.4			
St. 4	0–120			6.5	2.9			
St. 5	0–120			nd	3.4			
St. 6	0–120			11.4	2.4			
St. 7	0–120			20.9	3.4			
St. 8	0–120			nd	6.1			
St. 9	0–120			9.1	6.3			
St. 10	0–120			7.8	2.3			
St. 12	0–120			3.5	2.2			
St. 15	0–120			4.6	4.3			
			Mean POC flux	7.8	3.4 ± 1.5		7.1 ± 4.0	
Re-calculated results (SS)								
St. 1	0–120	3.3	244	4.8	2.0 ± 0.8		5.0 ± 0.7	
St. 2	0–120	2.2	358	4.3	2.6 ± 0.5		12.6 ± 0.9	
St. 3	0–120	3.6	306	5.3	2.3 ± 0.6		2.6 ± 0.8	
St. 4	0–120	2.2	179	6.5	3.9 ± 0.5	2.9[b]	4.8 ± 0.4	10.0[b]
St. 6	0–120	1.2	152	11.4	1.4 ± 0.3	2.4[b]	3.8 ± 0.3	5.0[b]
St. 7	0–120	1.8	141	20.9	2.3 ± 0.4	3.4[b]	6.8 ± 0.2	9.3[b]
St. 10	0–120	3.6	230	7.8	4.6 ± 0.8	2.3[b]	4.3 ± 0.4	3.9[b]
St. 12	0–120	2.0	105	3.5	2.1 ± 0.4	2.2[b]	1.4 ± 0.2	4.2[b]
St. 15	0–120	3.6	102	4.6	4.3 ± 0.8		1.3 ± 0.2	
			Mean POC flux	7.7	2.8 ± 1.8		4.7 ± 1.6	
			Mean POC flux w/adv. corr.		2.7 ± 1.4		6.0 ± 1.4	

[a] POC/^{234}Th(^{210}Po) ratio from sediment trap samples deployed at 100 m.
[b] Values corrected for advection. In the case of ^{234}Th, values correspond to Murray et al. (1996).

particles) for the upper 500 m at Stations # 10, 8 and 6 (Sta. RFZ was not considered due to scatter in the POC resulting from large-scale upwelling in this region). They obtained a rather robust correlation ($r^2 = 0.61$) between the ^{210}Po deficiency and POC, and suggested that scavenging by organic matter was the cause of the ^{210}Po deficiency. The actual ^{210}Po-derived POC export fluxes were not estimated.

We re-calculated the ^{234}Th–POC fluxes using the POC/^{234}Th ratio in the $>53\,\mu m$ size fraction of particles collected at the base of the euphotic zone. For the ^{210}Po/^{210}Pb approach,

Table 7
Published POC export fluxes from the Mediterranean Sea (MedFlux project) (Stewart et al., 2007a, b).

Station	Depth (m)	ST POC flux (mmol $m^{-2} d^{-1}$)	^{234}Th–POC flux (mmol $m^{-2} d^{-1}$)	^{210}Po–POC flux (mmol $m^{-2} d^{-1}$)
Sta 1: 5/Mar/2003	0–200		17.5 ± 11.8[a]	6.7 ± 1.2[a]
Sta 2: 7/May/2003	0–200		12.6 ± 4.3[a]	4.4 ± 2.0[a]
Sta 3: 11/May/2003	0–200		3.8 ± 1.5[a]	
Sta 4: 13/May/2003	0–200			7.0 ± 3.4[a]
Sta 5: 30/Jun–1/Jul/2003	0–200		4.7 ± 1.7[a]	4.8 ± 4.0[a]
Traps				
8/Mar/2003–3/May/2003 WC profiles from 7/May/03	200	2.2	4.2 ± 1.2[b]	1.2 ± 0.5[b]
16/May/2003–27/Jun/2003 WC profiles from 1/Jul/03	200	1.2	10.7 ± 2.1[b]	2.6 ± 0.3[b]

[a] POC/^{234}Th(^{210}Po) ratio measured in >70 μm particles from *in situ* pumps.
[b] POC/^{234}Th(^{210}Po) ratio from sediment trap samples deployed at 200 m.

Table 8
Published POC export fluxes from the Sargasso Sea (EDDIES project) (Buesseler et al., 2008).

Cruise/station	Depth (m)	^{234}Th–POC flux[a] (mmol $m^{-2} d^{-1}$)	^{234}Th–POC flux[b] (mmol $m^{-2} d^{-1}$)	^{210}Po–POC flux[b] (mmol $m^{-2} d^{-1}$)
E3 cruise				
EC	0–150	2.1 ± 0.7	1.5 ± 0.6	4.5 ± 2.4
Edge	0–150	1.8 ± 0.6	1.4 ± 0.5	3.5 ± 1.1
E4 cruise				
EC 1	0–150	1.6 ± 0.8	1.8 ± 0.5	3.3 ± 1.1
EC 2	0–150	1.1 ± 0.6	1.3 ± 0.9	1.5 ± 0.5
Traps				
Average fluxes (E3, E4)		1.2 ± 0.2		

EC: eddy centre.
Edge: station at the edge of the eddy.
[a] POC/^{234}Th ratio from sediment trap samples deployed at 150 m.
[b] POC/^{234}Th(^{210}Po) ratio measured in >53 μm particles from *in situ* pumps.

Table 9
Published PC export fluxes from the lee of Hawaii (North Tropical Pacific, Hawaii) (EFlux project) (Maiti et al., 2008; Verdeny et al., 2008).

Cruise/station	Depth (m)	Trap PC flux[a] (mmol $m^{-2} d^{-1}$)	POC/^{234}Th[b] (μmol dpm^{-1})	^{234}Th–PC flux[b] (mmol $m^{-2} d^{-1}$)	^{234}Th–PC flux[c] (mmol $m^{-2} d^{-1}$)	^{210}Po–PC flux[c] (mmol $m^{-2} d^{-1}$)
EFlux-I						
IN station	0–150	2.20 ± 0.23			0.87 ± 0.12	1.71 ± 0.16
OUT station	0–150	2.31 ± 0.26			1.24 ± 0.10	1.69 ± 0.16
EFlux-III						
IN station	0–150	1.54 ± 0.11	1.22 ± 0.03	0.65 ± 0.17	0.40 ± 0.08	1.58 ± 0.10
OUT station	0–150	1.52 ± 0.16	1.45 ± 0.05	0.76 ± 0.24	0.09 ± 0.05	1.67 ± 0.16

[a] Traps deployed at 150 m.
[b] POC/^{234}Th ratio measured in >53 μm particles from *in situ* pumps.
[c] Calculated using the inventory of PC.

no values were published for the POC/^{210}Po ratios, nor were the ^{210}Po–POC fluxes calculated by the authors. However, we obtained POC data from two size fractions of the *in situ* pumps, 0.7–53 μm and >53 um (M.A. Charette, pers. comm.), with which we could calculate the ^{210}Po–POC fluxes. As particulate ^{210}Po was only determined in the >0.7 μm particles, we could only use the POC/^{210}Po ratio in this size fraction. For comparative purposes, we also estimated the ^{234}Th–POC fluxes using the value of the POC/^{234}Th ratio in the >0.7 μm size fraction (Table 3).

2.3. Antarctic circumpolar current (Rutgers van der Loeff et al., 1997; Friedrich and Rutgers van der Loeff, 2002)

Rutgers van der Loeff et al. (1997) and Friedrich and Rutgers van der Loeff (2002) examined particle export from the surface ocean during a spring phytoplankton bloom in the Antarctic Circumpolar Current (ACC). Friedrich and Rutgers van der Loeff (2002) used ^{234}Th, ^{210}Pb and ^{210}Po as tracers for evaluating POC and biogenic silica (BSi) export from the upper 100 m. Measurements were made on three transects across the ACC, from the

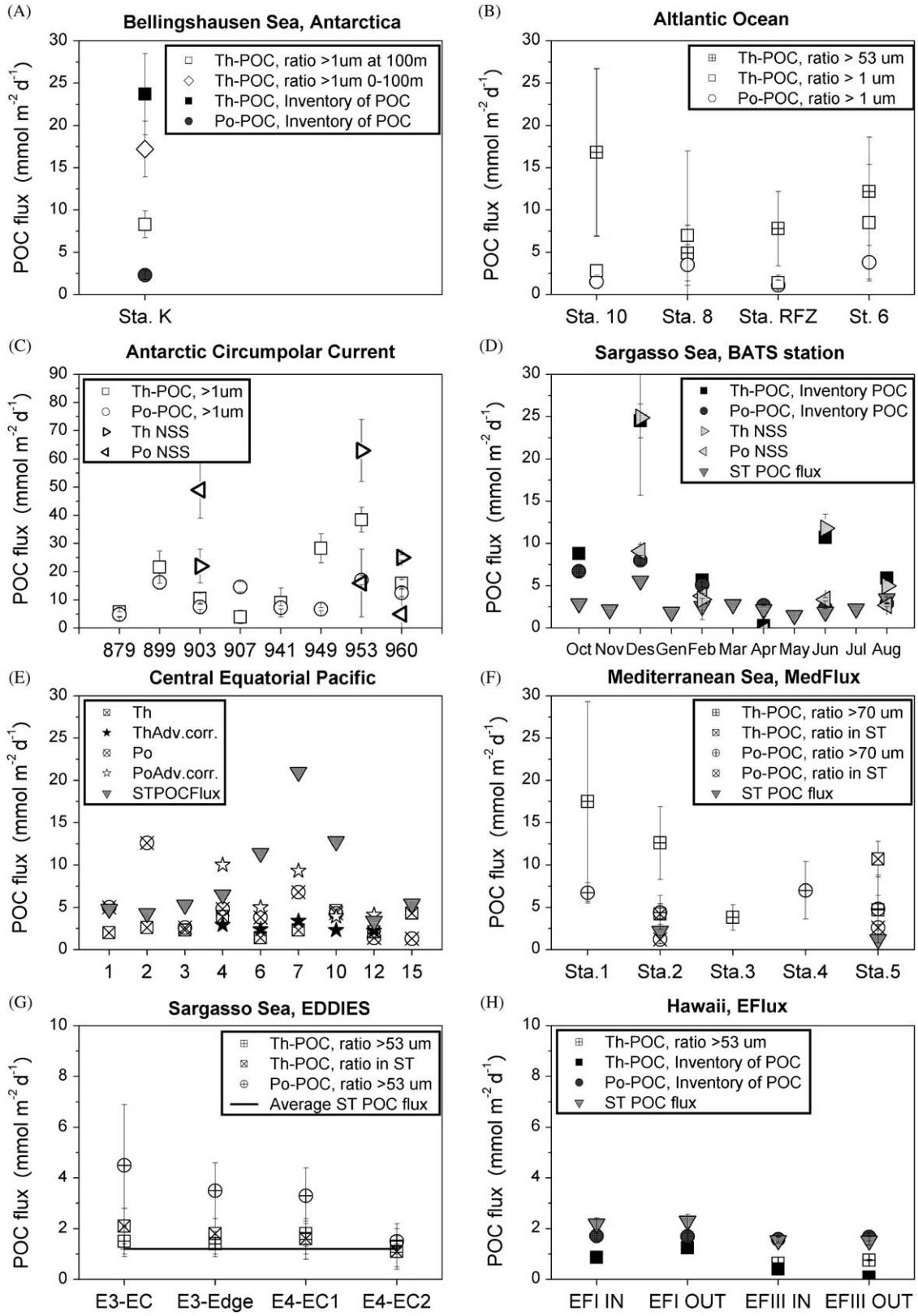

Fig. 2. Re-calculated POC export fluxes for each case study. Squares refer to ^{234}Th-POC estimates. Circles refer to ^{210}Po-POC estimates. Triangles and stars represent NSS and corrected for advection estimates, respectively. POC fluxes from sediment traps are represented with an inverted triangle. Note the change in scale in (C), (G) and (H).

Marginal Ice Zone (MIZ) to the Polar Front region (PFr): Transects 2, 5 and 11, corresponding to the beginning, middle and end of the austral spring, respectively. The particulate activities of ^{234}Th and ^{210}Po were obtained from filtering 50–250 L seawater samples through 1 μm filters. POC samples were obtained from filtering 1–2 L through GF/F filters.

In our re-calculation we considered 8 stations from their study (see Table 4), based on availability of the POC data. We used a SS approach for all stations and we additionally applied NSS conditions (Eq. (8)) at those sites that were sampled more than once in consecutive transects. We considered values for the POC/^{234}Th and POC/^{210}Po ratios for each station individually, corresponding to the >1 μm size fraction.

2.4. Sargasso Sea (Kim and Church, 2001)

In this study, ^{238}U–^{234}Th and ^{210}Pb–^{210}Po pairs were measured bi-monthly through the upper 500 m of the water column at the Bermuda Atlantic Time-Series Study (BATS) site in the Sargasso Sea. Sampling took place from October 1996 to August 1997. Dissolved and particulate seawater samples were obtained by filtration through 0.45 μm cartridge filters, of 20 L samples.

The POC export fluxes for SS and NSS conditions were re-calculated for both ^{234}Th and ^{210}Po approaches (Table 5). Due to the lack of primary data for calculating the POC/radionuclide ratios, we used the inventory of suspended POC in the water column from 0 to 150 m (data from Steinberg et al., 2001).

2.5. Central Equatorial Pacific (Murray et al., 1996, 2005)

The export flux of POC was measured in the Central Equatorial Pacific, as part of the US JGOFS Eq. Pac. study in 1992, using both ^{234}Th and ^{210}Po approaches with organic carbon measurements from suspended material and drifting sediment traps. Samples were collected in February–March 1992 from 12°N to 12°S at 140°W, during moderate El Niño conditions, with relatively warm surface water temperatures. Samples were also collected along a second survey in August–September 1992, during the development of a cold-tongue condition. Water column profiles were sampled from the surface to 250 m for dissolved, particulate (>0.45 μm) and total ^{234}Th, ^{210}Pb and ^{210}Po. Seawater samples of ~20 L were collected from Go-Flo bottles. The flux of particles was sampled using drifting sediment traps of the PIT design (Knauer et al., 1990). Particulate samples from traps deployed at 5–7 depths from 50 to 250 m were analysed in order to obtain the POC/radionuclide ratio in the sinking particles.

For this case study we focused on re-calculating the fluxes for Survey I (Table 6). Murray et al. (1996, 2005) applied advection corrections between 5°N and 5°S, where the vertical and meridional velocities were available (Chai et al., 1995). From the graphs in Murray et al. (2005) we could roughly estimate the amount of ^{210}Po that was advected vertically. However, we could not estimate the advective flux of ^{234}Th in Murray et al. (1996). Like the authors, we used a one-box model approach and the POC/radionuclide ratio measured in sediment trap samples. All fluxes have been calculated for the base of the euphotic zone (120 m) in the sampling area.

2.6. Mediterranean Sea (MedFlux project; Stewart et al., 2007a, b)

The goal of the MedFlux project was to understand the role of ballast in the vertical flux of organic matter in the mesopelagic zone. Samples were collected during four sampling cruises in the spring and summer of 2003 at the Dyfamed site in the Northwest Mediterranean Sea. ^{234}Th and ^{210}Po samples were collected in the water column at the beginning and end of two moored sediment trap deployments. The ^{234}Th activities (in the dissolved and particulate fractions) were measured using large volume *in situ* pumps. For ^{210}Pb–^{210}Po, 20 L samples were collected using Niskin bottles and filtered through 0.2 μm to separate particulate and dissolved fractions. POC was also measured in the filters and pre-filters from *in situ* pumps (1 and >70 μm, respectively). ^{234}Th, ^{210}Po and POC were also measured in sediment trap material collected in both a time-series and settling velocity mode (Peterson et al., 2005).

In MedFlux, both the ^{238}U–^{234}Th and ^{210}Pb–^{210}Po isotope pairs were applied in identical fashion at the same locations in time and space. The POC flux was estimated at 200 m from ^{234}Th and ^{210}Po water column deficits and the POC/^{234}Th and POC/^{210}Po on both >70 μm filterable particles and in sediment trap material (Table 7).

2.7. Sargasso Sea (EDDIES project, Buesseler et al., 2008)

The goal of the EDDIES project was to examine the impact of a mode water eddy on particle flux in the Sargasso Sea (Buesseler et al., 2008). Samples were collected during two sampling cruises (E3 and E4) in July and August 2005. The second cruise represented the second visit to the same eddy after one month. Samples for total ^{234}Th were collected along a series of transects through the eddy and at targeted stations on each cruise. The sampling methodology for ^{234}Th was based on 4 L samples, as described in Buesseler et al. (2001) and Benitez-Nelson et al. (2001), and high water column resolution of 18–20 depths per profile over the upper 1000 m. For ^{210}Pb and ^{210}Po, 8–10 L seawater samples were collected for total activities from 15 to 16 different depths over the upper 400–500 m at four stations. Three out of the four profiles were collected inside the eddy, and one at the edge. The analytical methods for ^{210}Pb and ^{210}Po were identical to those of Masqué et al. (2002).

For estimating the POC fluxes (Table 8), the POC/^{234}Th and POC/^{210}Po ratios were both determined on the >53 μm size particles collected via *in situ* pumping from 120 to 150 m depth. The POC/^{234}Th ratios were also measured in sediment trap particles from below the euphotic zone.

2.8. North Tropical Pacific, Hawaii (E-Flux project; Maiti et al., 2008; Verdeny et al., 2008)

The E-Flux project was conducted to investigate the physical, biological and biogeochemical characteristics of cold-core cyclonic eddies that form in the lee of the Islands of Hawaii (Benitez-Nelson et al., 2007; Benitez-Nelson and McGillicuddy, 2008). The E-Flux sampling scheme consisted of three sampling cruises, each lasting approximately 3 weeks, that took place within a 6-month sampling period. These cruises sampled two distinct mesoscale eddies during different physical and biological stages of evolution, with Cyclone *Noah* sampled during E-Flux I (November 2004) and Cyclone *Opal* sampled during E-Flux III (March 2005) (Dickey et al., 2008; Kuwahara et al., 2008; Nencioli et al., 2008). Sampling for ^{234}Th was conducted along several transects through the eddies, in a star shape. High-resolution sampling of 4 L samples for ^{234}Th analysis was achieved between 0 and 1000 m depth (Maiti et al., 2008). For ^{210}Pb and ^{210}Po, 10 L samples were collected from 10 depths from the surface to 500 m depth, both at stations inside the eddy (IN stations) and in surrounding waters (OUT stations) (Verdeny et al., 2008). Particulate carbon (PC) was measured in three particulate size fractions from *in situ* pumps (1, 10 and 53 μm) and throughout the water column on small volume samples (1 μm). Microscope examinations of phytoplankton biomass showed little evidence of carbonate bearing organisms relative to diatoms; therefore the PC measured here was taken to be mainly composed of organic carbon (Brown et al., 2008; Landry et al., 2008).

The ^{234}Th-derived PC fluxes were calculated using the PC/^{234}Th ratio measured in the >53 μm size particles from 150 m depth.

Because the PC/^{210}Po ratio was not determined in this study due to the decay of ^{210}Po within the particulate samples at the time of analysis, the ^{210}Po-derived C fluxes were estimated using suspended water column PC and the residence times of ^{210}Po over the depth interval of interest (0–150 m). For comparative purposes, the ^{234}Th–PC fluxes have also been estimated using the inventory of PC (Table 9).

3. Results

For an appropriate comparison of the ^{234}Th–POC and ^{210}Po–POC flux estimates, one should consider estimates that have been obtained using similar approaches. For example, in the Bellingshausen Sea, at BATS (Sargasso Sea) and in Hawaii (E-Flux) we compare estimates obtained through the inventory of POC and the residence time of particulate ^{234}Th and ^{210}Po. In the Atlantic Ocean and the ACC, we compare fluxes calculated using the value of the POC/radionuclide ratio in the $>1\,\mu m$ fraction. We compare estimates obtained using the POC/radionuclide ratio at >53 or $70\,\mu m$ particles for EDDIES (Sargasso Sea) and at the Dyfamed station (Mediterranean Sea), and using the POC/radionuclide ratio in sediment trap (ST) particles also in the Mediterranean Sea and in the Central Equatorial Pacific.

We note that the studies under review comprise sampling sites that may differ greatly in productivity, particle composition and hydrographical regimes. Nevertheless, our purpose in comparing ^{234}Th and ^{210}Po as POC tracers does not involve a site-to-site comparison in terms of quantitative fluxes. Here, we carry out two different types of comparisons. First we compare model fluxes, both from ^{234}Th and ^{210}Po, with fluxes recorded directly in sediment traps. Second we compare model ^{234}Th–POC fluxes with model ^{210}Po–POC fluxes for all stations under review.

3.1. Comparing model fluxes with sediment trap fluxes

At least five of the eight studies under review provided us with the necessary data for carrying out a comparison between SS model fluxes and sediment trap fluxes. The model ^{234}Th–POC and ^{210}Po–POC flux estimates, obtained using the inventory of suspended POC, are compared with the POC fluxes recorded in sediment trap samples (data from BATS and Hawaii) in Fig. 3A. An analogous analysis can be done comparing model fluxes obtained using the POC/radionuclide ratio in large particles (>53 or $70\,\mu m$) from the *in situ* pumps with sediment trap fluxes (Fig. 3B, data from EDDIES, in the Sargasso Sea, and the Mediterranean Sea). We finally compare model fluxes using the ratio in sediment trap

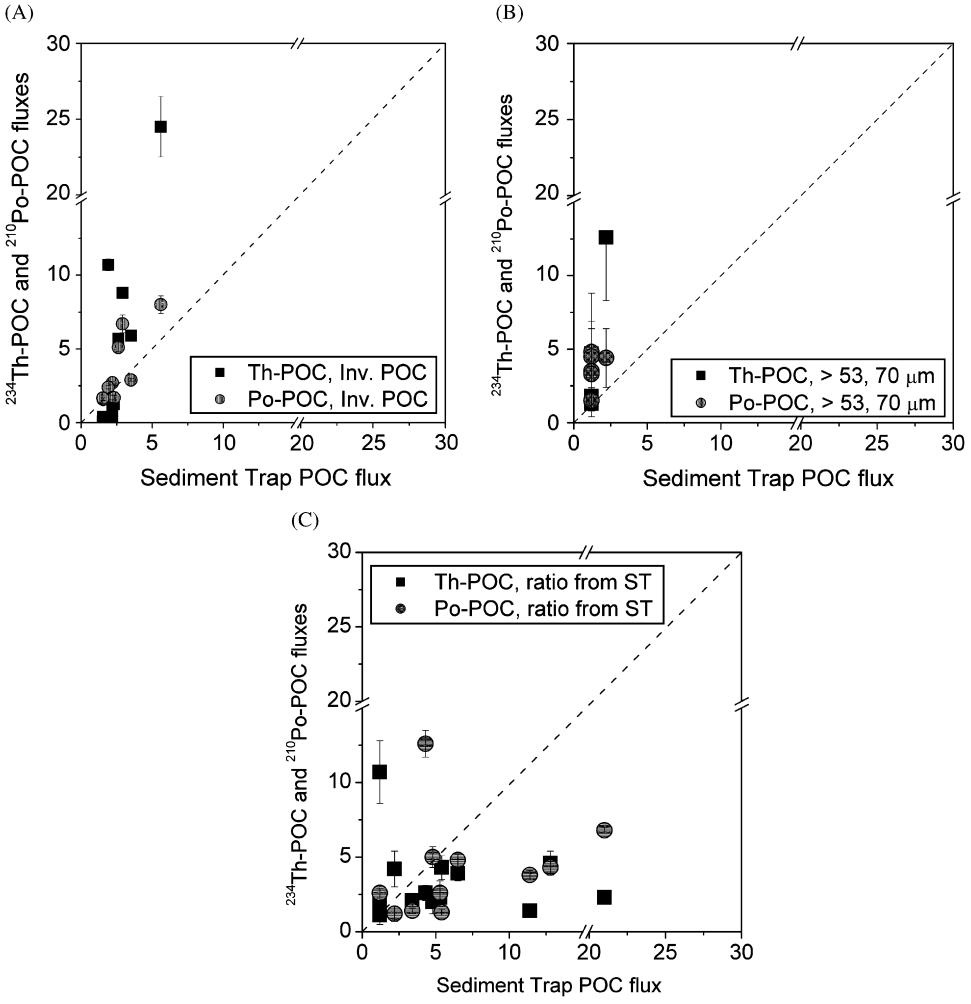

Fig. 3. A comparison of the modelled SS POC fluxes using ^{234}Th and ^{210}Po with the POC fluxes recorded in sediment traps: (A) modelled fluxes obtained using the inventory of suspended POC (data from Sargasso Sea-BATS and Hawaii); (B) modelled fluxes obtained using the POC/radionuclide ratio in large particles collected using in situ pumps (data from Sargasso Sea-EDDIES and Mediterranean Sea); (C) modelled fluxes obtained using the POC/radionuclide ratio in sediment trap samples (data from Central Equatorial Pacific, Sargasso Sea-EDDIES and Mediterranean Sea).

samples with the sediment trap fluxes themselves (Fig. 3C, data from the Equatorial Pacific, EDDIES and the Mediterranean Sea).

3.2. Comparing model flux estimates

For the study in the Bellingshausen Sea (see Table 2, Fig. 2A), the ^{234}Th–POC and ^{210}Po–POC fluxes calculated using the inventory of POC in the upper 100 m were 24 ± 5 and 2.3 ± 0.5 mmol m^{-2} d^{-1}, respectively. In the Atlantic Ocean (Table 3, Fig. 2B), the ^{234}Th–POC and ^{210}Po–POC flux estimates calculated using the ratio in particles >1 μm gave up to 2-fold higher results for ^{210}Po.

In the ACC (Table 4, Fig. 2C), the SS ^{234}Th–POC and ^{210}Po–POC flux estimates agreed within a factor of 1.5, with slightly higher ^{234}Th-derived estimates in 5 out of 8 stations. For stations 949 and 953, the ^{234}Th–POC fluxes were larger by a factor of more than 4 and 2, respectively. Only Station 907 showed a larger ^{210}Po–POC estimate, by almost 4-fold.

At BATS (see Table 5, Fig. 2D), the ^{234}Th–POC and ^{210}Po–POC fluxes gave similar results, within a factor of 2, with slightly higher ^{234}Th estimates for half of the stations. For December 96 and June 97, the ^{234}Th–POC fluxes were larger by 3- and almost 5-fold, respectively, whereas in April 97 the ^{210}Po–POC estimate was 2.7 mmol C m^{-2} d^{-1} compared to an almost non-existent flux derived from ^{234}Th. The NSS fluxes were generally larger using the ^{234}Th approach, but were within a factor of 3.5 of the ^{210}Po estimates.

In the Equatorial Pacific (Table 6, Fig. 2E) the re-calculated ^{234}Th- and ^{210}Po-derived POC fluxes without the advection correction gave similar results, within a factor of 3, with slightly higher ^{210}Po-derived estimates at the stations north of the equator (Sta. 1, 3, 4 and 7) and slightly higher ^{234}Th estimates at the stations south of the equator (Sta. 10, 12 and 15). Only for Sta. 2 the ^{210}Po–POC estimates were substantially higher, by almost 5-fold, than the ^{234}Th estimates. Comparing the flux estimates obtained with advection corrections (Sta. 4–12), the ^{210}Po–POC estimates were larger than the ^{234}Th estimates by 2–3-fold.

The POC fluxes at the Dyfamed site in the Mediterranean Sea are shown in Table 7 and Fig. 2F. Notice that we refer to stations in order to identify the timing of sampling at a particular site. Using the ratio in >53 μm particles, ^{234}Th–POC fluxes were almost a factor of 3 higher than the ^{210}Po–POC estimates for Sta. 1 and Sta. 2. Both estimates were comparable at Sta. 5, and ^{210}Po–POC fluxes were larger by almost 2-fold at Sta. 4. Comparing the flux estimates derived from the use of the C/radionuclide ratios measured in sediment traps, the ^{234}Th–POC estimates were a factor of 4 larger than the ^{210}Po–POC flux estimates.

The results from the EDDIES project in the Sargasso Sea are provided in Table 8 (Fig. 2G). For the POC flux estimates using the ratio in particles >53 μm, we found larger ^{210}Po–POC fluxes compared to the average ^{234}Th–POC flux at 150 m by a factor of 3 in the E3 cruise and a factor of 2 during the E4 cruise. The ^{234}Th–POC fluxes obtained using the ratio measured in sediment trap particles were not statistically different from the fluxes using the ratio in >53 μm particles.

The PC flux results from the E-Flux project off Hawaii are given in Table 9 (Fig. 2H). Comparing PC fluxes using the inventory of PC in the water column, we found comparable fluxes within a factor of 2 of slightly larger ^{210}Po–PC estimates for E-Flux I. For E-Flux III, the ^{210}Po–PC fluxes were 4-fold larger than the corresponding ^{234}Th–derived at the IN station and averaged 1.67 mmol C m^{-2} d^{-1} at the OUT station compared to an almost no flux obtained using ^{234}Th.

In Fig. 4 we plotted the ^{234}Th- and ^{210}Po-derived POC flux estimates for all the data considered in this review. In general,

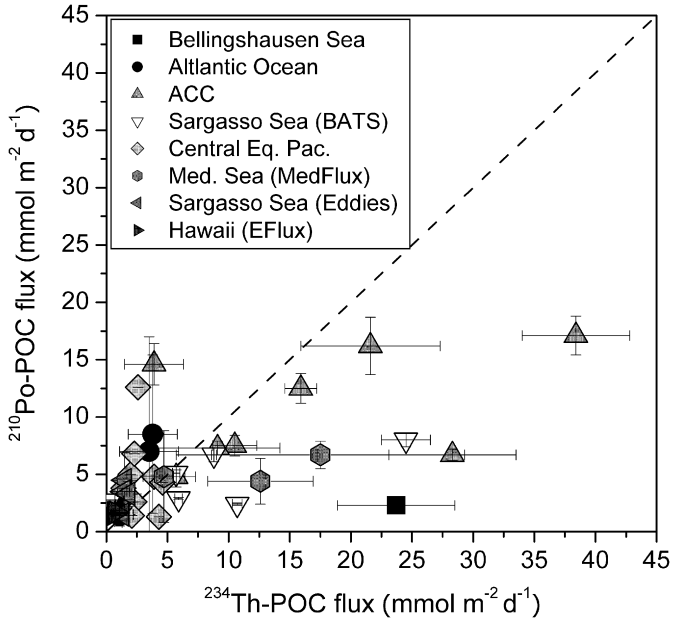

Fig. 4. Plot of the ^{210}Po-POC flux estimates versus the ^{234}Th-POC flux estimates for every study considered under review. All values in SS.

there is a trend for higher ^{234}Th–POC flux estimates relative to those obtained using the ^{210}Po approach. Indeed, the ^{234}Th–POC flux estimates comprise a broader range of values, from 0 up to 40 mmol C m^{-2} d^{-1}, versus the narrower range of the ^{210}Po–POC flux estimates, from 0 to less than 20 mmol C m^{-2} d^{-1}.

In Fig. 5 we separately considered the four different approaches that have been used to estimate the POC fluxes. One can clearly see that POC flux estimates derived from the use of the inventory of POC and the particulate residence time of the radionuclides tends to give larger ^{234}Th-derived estimates (Fig. 5A). A similar trend is found when comparing estimates obtained using the POC/radionuclide ratio in >1 μm particles (Fig. 5B), although in 9 out of 12 stations both estimates compare reasonably well. In Figs. 5C and D the comparison is made between flux estimates obtained using the ratio in large particles from *in situ* pump filtration (>53 or 70 μm) and the ratio in sediment trap particles, respectively. No clear trend is observed in these two plots at first sight. However, the ^{210}Po–POC fluxes measured in the Mediterranean Sea give lower values relative to the ^{234}Th–POC, which could be related to a more effective scavenging of ^{234}Th onto lithogenic material present in the water column from the frequent atmospheric deposition of Saharan dust in the western Mediterranean (see Section 4). In the remaining data, there is a tendency towards slightly larger ^{210}Po–POC flux estimates relative to those using ^{234}Th (Figs. 5C and D).

4. Discussion

4.1. Comparing ^{234}Th- and ^{210}Po-derived fluxes to sediment traps

Despite the limited set of available data for carrying out the comparison, there are several trends. For small fluxes (i.e. <5 mmol C m^{-2} d^{-1}) both ^{234}Th and ^{210}Po model flux estimates are comparable to the sediment trap fluxes, independent of the approach used for obtaining the model fluxes. For higher fluxes and when using the inventory of POC (Fig. 3A), there is a tendency towards larger model fluxes versus sediment trap fluxes, for both ^{234}Th and ^{210}Po. If we assume that the particles collected in

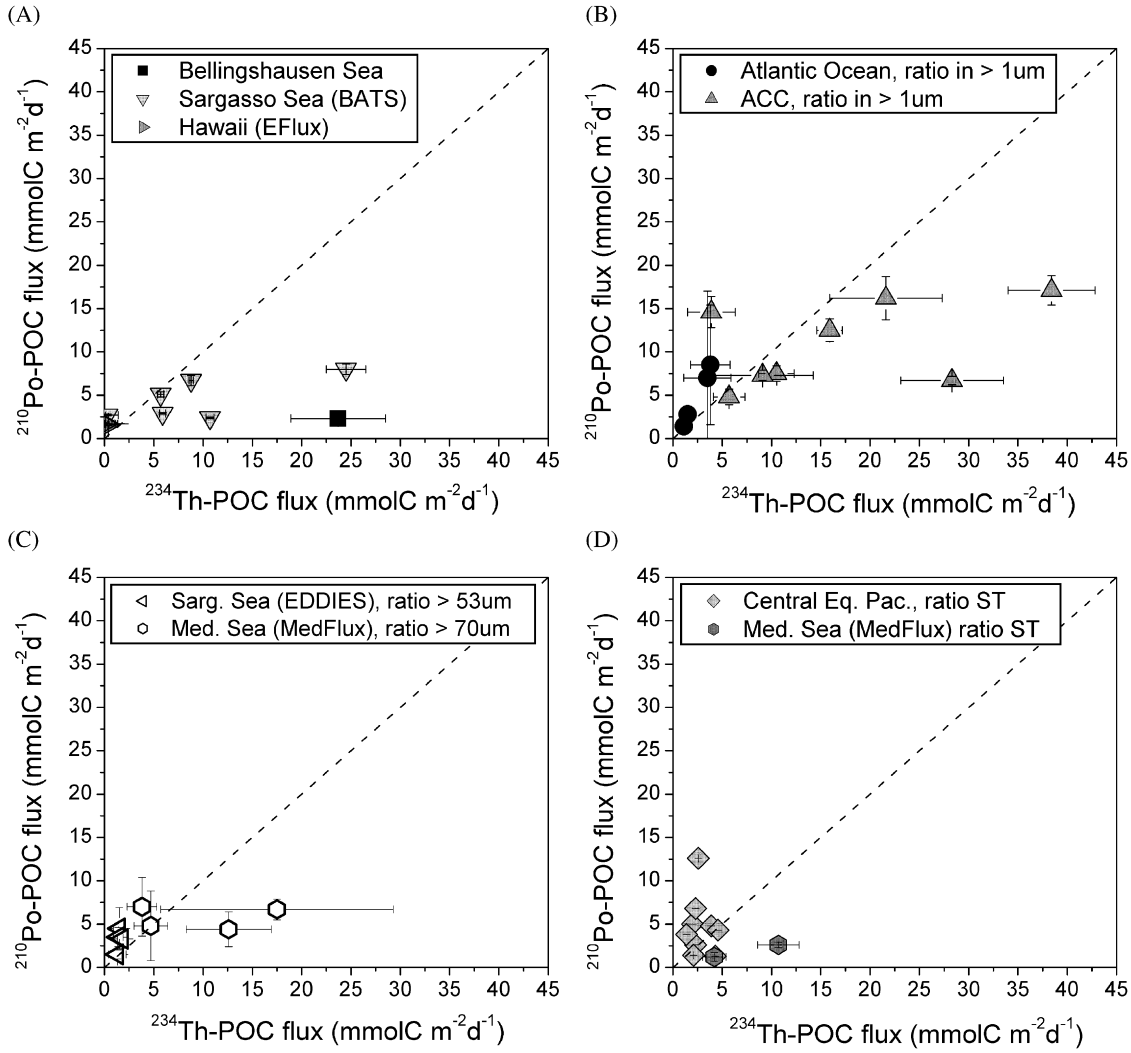

Fig. 5. Plot of the ^{210}Po-POC flux estimates versus the ^{234}Th-POC flux estimates in the four different approaches used for obtaining the POC fluxes: (A) using the inventory of the POC; (B) using the POC/radionuclide ratio in the $>1\,\mu m$ particles; (C) using the ratio in >53 (70) μm particles; (D) using the ratio in sediment trap particles.

sediment traps create the deficits in the water column recorded by ^{234}Th and ^{210}Po, the higher model fluxes obtained using the inventory of POC is likely because this calculation takes into account all suspended particles (namely $>1\,\mu m$). In other words, not all of the organic carbon containing particles used to determine the POC inventory are exported. Rather, suspended particles may be recycled before they reach the sediment traps.

We also found higher model POC fluxes versus sediment trap fluxes using the ratio in large particles from the *in situ* pumps (Fig. 3B). The pumps collect particles that are present in the water column whether or not these particles contribute to the sinking flux. The fact that we obtain higher model fluxes in this case can be related to: (i) *in situ* pumps collect $>53\,\mu m$ (or $70\,\mu m$) particles, that can be either sinking or buoyant; (ii) the sinking particles collected in the sediment traps might have been more affected by remineralization on their way into the trap.

From the comparison of sediment trap fluxes with model fluxes using the POC/radionuclide ratio from sediment trap samples (Fig. 3C), we observe a trend towards larger sediment trap fluxes for almost all cases. This could indicate that in general sediment traps tend to overcollect with respect to the measured disequilibria (Buesseler, 1991). On the other hand, model fluxes could be underestimated by not considering physical processes such as upwelling, especially in the Central Equatorial Pacific where, for instance, higher ^{210}Po-derived POC fluxes relative to sediment traps occurs at St. 2. The largest difference between ^{234}Th-derived POC flux and the sediment trap flux is at the Dyfamed site where ballasting may be an issue (see detailed discussion in Cochran et al., 2009, this issue).

4.2. *Importance of half-lives of ^{234}Th and ^{210}Po*

When comparing POC fluxes derived from ^{234}Th and ^{210}Po, we must consider one of the greatest inherent differences that exist between the two tracers: their half-lives. The half-life of ^{210}Po is about 4.5 times that of ^{234}Th (138.4 and 24.1 d, respectively). As such, the distributions of ^{234}Th and ^{210}Po in the water column integrate changes over different time scales. Both tracers give a weighted integration of the changes in the water column, such that the changes that occurred just prior to the sampling time are weighted more heavily than those that occurred further in the past. However, averaging export over longer time scales would tend to smooth out episodic events and may give a lower mean. For example, ^{210}Po integrates the flux over a longer period of time that may include a period of lower flux previous to a bloom,

whereas ^{234}Th deficits may reflect a more rapid change in the water column during the bloom itself. This inherent difference between the tracers could explain the generally higher ^{234}Th–POC fluxes versus ^{210}Po–POC fluxes observed (Fig. 4), as sampling is usually undertaken when a bloom is more likely to occur.

The difference in half-lives is also relevant when applying a non-steady state approach. For most studies, a 1-D steady state model is the only chance for estimating particle fluxes, although this simple model may not adequately characterize the distribution of radionuclides as a function of time and space. An improvement relies in the use of a non-steady state model, which would be more sensitive to changes in the water column over time (Savoye et al., 2006). Non-steady state models require repeated sampling of a given station over a short period of time appropriate to the half-life of the tracer. A time interval of 2–3 weeks would be best for ^{234}Th, whereas for ^{210}Po, a time interval of 2–3 months would be sufficient. As a result, ^{234}Th could be better used to record short-term changes in the water column, while ^{210}Po could be used to record longer-term (e.g. seasonal) changes in export fluxes. Unfortunately, we could not calculate NSS flux estimates for the studies included here to demonstrate how SS and NSS flux calculations differ.

The effects of upwelling, advection and lateral transport can also play an important role in the activity profiles of ^{234}Th and ^{210}Po. Again, it must be evaluated whether the physical characteristics of the water column influence the ^{234}Th and ^{210}Po profiles, and their disequilibrium, in the same way and to the same extent. The effect of upwelling is to bring deep waters to the surface. Waters from below the euphotic zone usually have higher activities of ^{210}Po (with respect to ^{210}Pb) and ^{234}Th tends to be in equilibrium or closer to equilibrium with ^{238}U (or higher than ^{238}U due to remineralization). Therefore, when deeper waters are upwelled the resulting calculated export fluxes are most commonly underestimated. For example, in the Central Equatorial Pacific, especially near the equator, the ^{210}Po–POC fluxes were enhanced by about 30–70% when vertical advection corrections were considered (Murray et al., 2005). In the same area, Buesseler et al. (1995) also found that ^{234}Th fluxes were 25–35% higher when an upwelling term was included. At Station RFZ in the Central Equatorial Atlantic, Charette and Moran (1999) reported qualitatively high upward flux of deep waters, although the strength of the upwelling could not be determined. However, in their transect through the mid-Atlantic, the highest rate of productivity was found at station RFZ, despite the relatively low calculated POC fluxes. The authors attributed this to the lack of upwelling corrections. In spite of the evidence that physical processes affect the modelled fluxes, more studies should be conducted where transport velocities are also measured to evaluate how ^{234}Th and ^{210}Po (and ^{210}Pb) are affected by the physical processes ongoing at a given sampling area.

Another parameter that is influenced by the half-lives of ^{234}Th and ^{210}Po, and their *in situ* production rate, is the depth of integration. One can integrate the water column deficiency of ^{234}Th and ^{210}Po and calculate the fluxes for any desired depth. Most studies focus on determining the production exported from the euphotic zone. When using the ^{238}U–^{234}Th approach, the depth of integration is usually easy to determine and is taken at the depth where ^{234}Th reaches equilibrium with ^{238}U. For the ^{210}Pb–^{210}Po approach, the choice of the depth of integration may not be so clear nor unique: ^{210}Po rarely reaches secular equilibrium with ^{210}Pb in the upper few hundred metres of the water column. This is due to the longer half-life of ^{210}Po and the fact that ^{210}Pb is also particle reactive, although to a lesser extent and in a different manner to its grand-daughter. The profiles of ^{210}Pb and ^{210}Po must, therefore, be compared to the distribution of other parameters that might help decide the depth of integration, e.g. by comparing these profiles to the ^{238}U–^{234}Th profiles, or taking the depth of integration as the base of the euphotic zone determined by light or thermocline.

In order to better characterize the distribution of the radionuclides in seawater, higher vertical sampling resolution is recommended, especially in the upper 500 m of the water column, to better constrain the deficiencies of ^{234}Th and ^{210}Po with respect to their parent nuclides and therefore better constrain the fluxes. For instance, in the study carried out in the ACC, the sampling resolution was very low for all stations with only 3 or 4 sampling depths from the surface to 200 m. The authors integrated radionuclide deficiencies in the upper 100 m, but in some cases ^{234}Th was still depleted at deeper depths (see Rutgers van der Loeff et al., 1997 and/or Friedrich and Rutgers van der Loeff, 2002). In the Bellinghausen Sea (Shimmield et al., 1995) and the Atlantic Ocean (Charette and Moran, 1999; Sarin et al., 1999), between 6 and 9 depths were sampled in the upper 500 m. In contrast, in the Central Equatorial Pacific (Murray et al., 1996, 2005) 9 depths were collected between the surface and 250 m depth, and in the Sargasso Sea, Kim and Church (2001) achieved a high sampling resolution comprised of 12–14 depths per profile down to 500 m. In the EDDIES and E-Flux projects, even higher resolution was accomplished: 15–16 sampling depths over the upper 400–500 m using small volume sampling techniques (4 L for ^{234}Th and 8–10 L for ^{210}Po). In the Mediterranean Sea (Stewart et al., 2007a, b), between 5 and 8 depths were sampled in the upper 200 m for both ^{234}Th and ^{210}Po.

4.3. Particle affinity

An important characteristic that distinguishes these tracers is their different biogeochemical behaviour and particle affinities, although ^{234}Th and ^{210}Po are both highly particle reactive. ^{234}Th is known to adsorb very effectively on the surface of particles (Santschi et al., 2006), whereas ^{210}Po is believed to behave in a manner similar to sulphur and is thus prone to bioaccumulation (Stewart and Fisher, 2003a, b). The differences in particle reactivity lead to different behaviours of the elements in seawater, especially in the upper water column, where most particles are produced and where recycling of organic matter is more intense. In addition, ^{234}Th and ^{210}Po are recognized to have different degrees of affinity depending on the type of particle (e.g. Stewart et al., 2007a, b).

^{234}Th–POC- and ^{210}Po–POC-derived fluxes are similar when fluxes are low, $<5\,\mathrm{mmol\,C\,m^{-2}\,d^{-1}}$ (see Fig. 5). Differences between the two methods become increasingly apparent when fluxes increase, probably due to differences in relative particle reactivity. When fluxes are calculated using the inventory of POC (Fig. 5A), the higher ^{234}Th–POC fluxes may be explained by a shorter residence time of ^{234}Th in the upper water column and, inversely, a longer residence time of ^{210}Po due to more efficient recycling together with organic matter. ^{234}Th is, therefore, more efficiently exported. Indeed, in the Bellingshausen Sea, Shimmield et al. (1995) suggested that the larger ^{234}Th–POC flux estimate compared to the ^{210}Po–POC was due to a large amount of lithogenic particles present in the water mass resulting from ice melting. Lithogenic particles would scavenge ^{234}Th more effectively than ^{210}Po, thus resulting in a larger ^{234}Th deficit and a larger ^{234}Th-derived POC flux. Shimmield et al. (1995) also related the differences in the fluxes to the residence times of the radionuclides in the mixed layer which was 10 times larger for ^{210}Po compared to ^{234}Th suggesting a rapid and efficient removal of ^{234}Th on sinking particles in contrast to ^{210}Po.

Larger ^{234}Th–POC than ^{210}Po–POC fluxes are also obtained when comparing estimates obtained using the POC/radionuclide

ratio in >1 μm particles (Fig. 5B), and similarly using the ratio in particles >53 μm (or 70 μm) (Fig. 5C) and the ratio measured in sediment trap samples (Fig. 5D). In the ACC, Friedrich and Rutgers van der Loeff (2002) reported blooms characterized by large particles, mainly diatoms, which might have been responsible for the larger ^{234}Th scavenging in this area relative to ^{210}Po. The ACC study used a model based on the different affinities of ^{234}Th and ^{210}Po for particles and hypothesized that ^{210}Po was mostly adsorbed onto POC and had little to no affinity for BSi. ^{234}Th was found to have affinity for both types of particulate material but demonstrated a larger affinity for BSi than POC.

Diatom blooms were also observed in mesoscale features such as eddies in the Sargasso Sea, but the absolute measured fluxes were very low and, if anything, were slightly larger when using the ^{210}Po approach (Buesseler et al., 2008). In the Equatorial Pacific, low fluxes were also reported but with a biological community comprised of small phytoplankton. Much of the organic carbon produced was in the form of DOC. In this region, there was a tendency towards slightly larger ^{210}Po–POC fluxes. The fluxes in the Mediterranean Sea, either using the >70 μm ratio or the ratios in sediment trap samples, were larger for ^{234}Th–POC than ^{210}Po–POC, similar to the Bellingshausen Sea. This could be related to a more effective scavenging of ^{234}Th onto lithogenic material present in the water column from the frequent atmospheric deposition of Saharan dust in the western Mediterranean.

Murray et al. (1996, 2005) examined the relationship between POC, ^{234}Th and ^{210}Po in particulate samples and obtained a satisfactory correlation using logarithmic values ($r^2 = 0.88$) between ^{234}Th and POC measured in sediment traps. They also found that POC/^{234}Th ratios in suspended particles (from MULVFS *in situ* filtration) were significantly larger than in trap samples, and suggested that recycling affects C and Th differently. Murray et al. (2005) evaluated the relationship between ^{210}Po and organic carbon in suspended and sediment trap particles. Without considering logarithmic values, they found a good correlation ($r^2 = 0.64$) (indicating better correlation between POC and Po than with Th) and little difference between the two particle types. From the consistency of the POC/^{210}Po ratio in MULVFS particles they suggested that these elements are recycled in a similar manner with little fractionation.

In general, the analysis presented here supports the hypothesis that ^{234}Th is more effectively scavenged by inorganic matter than ^{210}Po. From the different biogeochemical behaviour between ^{234}Th and ^{210}Po we conclude that ^{234}Th is expected to trace total mass flux (or total carbon) and ^{210}Po to trace POC (or organic matter) more specifically. If Po is recycled in the water column in a similar way to POC, this would reinforce its more specific use as a flux tracer for organic matter.

4.4. The POC/radionuclide ratio

Once the ^{234}Th or ^{210}Po flux from the upper water column is estimated, it can be used as a proxy for elemental particle flux by simply multiplying ^{234}Th or ^{210}Po export on sinking particles by the element/radionuclide ratio measured on the same sinking particles. For POC this would mean that the flux of POC equals the radionuclide flux times the POC/radionuclide ratio (Buesseler et al., 1992). This is an empirical approach that has inherent strengths and limitations that have been recently reviewed in detail for ^{234}Th by Buesseler et al. (2006). Briefly, variations in POC/^{234}Th can result from a variety of geochemical and biological processes, as well as sampling method. Sampling methods (e.g. using water column POC standing stock and radionuclide residence time) clearly bias results because the POC/radionuclide ratio is not specific to sinking particles. Even with an accurate estimate of radionuclide deficit, any variation in POC/radionuclide ratio may lead to over/underestimating the true POC flux. Therefore, Buesseler et al. (2006) state that studies must have site and depth specific POC/radionuclide data collected over the same time-scale as the integration time of the tracer the study is employing.

The main controversial point here lies in the choice of method for sampling the truly sinking particulate material. Usually, the particles >53 μm (or 70 μm) are considered to contribute to the sinking flux (usually compared to the smaller particles 1–53 or 1–70 μm). However, the POC/radionuclide ratio can also be determined in sediment trap samples, as these devices are meant to truly collect the settling particles, such as aggregates. However, a series of problems/limitations exist for both sampling methods. Concerning filtration, *in situ* pumps are questioned as a method for collecting sinking particles as there is no method to discern between sinking and suspended matter collected on filters and pre-filters. Niskin samples are believed to collect zooplankton that is not contributing to the sinking flux (e.g. Liu et al., 2005), but can greatly affect the value of the POC/radionuclide ratio. On the other hand, the collection efficiency of sediment traps can be affected by hydrodynamic problems, swimmer contamination and selective trapping of a given particle type (Gardner, 2000; Peterson et al., 2005; Buesseler et al., 2007). Neutrally buoyant floating sediment traps (Buesseler et al., 2000, 2007) may help resolve hydrodynamic problems associated with moored traps, but they have yet to be routinely deployed.

Buesseler et al. (2006) pointed out that the value of the POC/^{234}Th ratio might vary greatly with depth and size of the particle. In the Bellingshausen Sea, at Station K, Shimmield et al. (1995) reported values of the POC/^{234}Th ratio that clearly decreased with depth. The re-calculated POC export at that site using the value of the POC/^{234}Th ratio at 100 m (6.5 μmol dpm^{-1}) is 8.3 mmol C m^{-2} day^{-1}, a factor of 2 smaller than the original estimate using an average ratio for the 0–100 m interval. In this paper, we assert that the ratio at the base of the euphotic zone should be more representative of the sinking exported particles.

In the Atlantic Ocean, Charette and Moran (1999) reported a trend of decreasing POC/^{234}Th ratio with decreasing particle size, such that the ^{234}Th–POC fluxes increase by an average factor of 4 when using the ratio in the >53 μm particles compared to the ratio in >1 μm. On the other hand, in the ACC, Rutgers van der Loeff et al. (1997), based on literature data on C and ^{234}Th in suspended matter and trap material, stated that the POC/^{234}Th ratio of the material that is exported from the euphotic zone, i.e. caught in sediment traps, amounted to 30–60% of the ratio in suspended particulate material. In this case, the ^{234}Th–POC estimated from the ratio in >1 μm particles would correspond to a lower limit. Unfortunately, there is little or no information on how the POC/^{210}Po ratio varies with depth and size. Thus, no such comparison can be made.

We suggest that the particulate radionuclides and organic carbon (or any other parameter for which export is to be estimated) should be measured on the same type of sample or, better yet, taken from the same sample. Different sampling mechanisms can lead to biases in estimating the exported fluxes of the radionuclides or carbon. For example, in the ACC the POC was measured from 1 to 2 L bottle samples, and ^{234}Th and ^{210}Po from separate 50–250 L bottle samples. Kim and Church (2001) obtained the POC measurements from 1 to 2 L bottle samples collected during routine BATS sampling, and the radionuclides were measured from 30 L samples collected at the same time. Both of these methods introduce possible differences in the POC/radionuclide ratios. More specifically, DOC adsorption onto filters is more important for small volume filtration than large volume

filtration (Moran et al., 1999; Liu et al., 2005), and it has also been suggested that high pressure during filtration (e.g. during *in situ* pump filtration) may break particles and force POC through the filter.

5. Conclusions

We revised and presented all historical data on the simultaneous application of ^{210}Po and ^{234}Th as POC flux proxies in order to: (1) compare the results from applying these two proxies; (2) obtain new insights from this comparison, analysing the reasons why the flux estimates differed or gave similar values; (3) evaluate to what extent the combined use of both tracers provides complementary information: and, finally, (4) give new insights to help decide which tracer is more suitable under specific oceanographic conditions. The two tracers studied here, ^{234}Th and ^{210}Po, have proven to be useful tracers for POC export production. However, the two greatest inherent differences that exist between the two tracers (half-life and scavenging affinity) make them useful in different and complementary ways.

Their different half-lives enable us to study export production rates over different time scales. ^{234}Th is proven to be best used for short-term flux determination whereas ^{210}Po may be more suitable for seasonal flux estimates. If one is interested in applying a NSS approach, the temporal resolution should be different for each tracer as well, i.e. a time interval between consecutive samplings of 2–3 weeks for ^{234}Th and up to 2–3 months for ^{210}Po. The difference in half-lives may also play an important role in areas strongly influenced by lateral advection and upwelling of deep waters. Evidence that physical processes affect the modelled fluxes have been documented but more work needs to be conducted in order to evaluate whether the physical processes affect ^{234}Th and ^{210}Po in a similar quantitative way. Additionally the production functions of ^{234}Th and ^{210}Po in the water column (^{238}U and ^{210}Pb, respectively) are governed by different mechanisms, allowing lateral advection and vertical upwelling to be investigated, and provide different information on the water column dynamics.

The different biogeochemical behaviour of ^{234}Th and ^{210}Po, and their preference for specific types of particles, although not yet fully deciphered, is a potential advantage. Our analysis of the compiled dataset presented in this study provides evidence that ^{234}Th displays a larger affinity for inorganic particulate matter and is expected to trace total mass flux (or total carbon). On the other hand, ^{210}Po seems to directly trace at least certain components of POC, given its tendency to act like sulphur and to be recycled in the water column in a manner similar to POC.

The differences that ^{234}Th and ^{210}Po present in half-lives, particle affinity and production functions are thus great advantages for studying changes in the water column biological dynamics, quantifying export production and better understanding the physical processes ongoing at a given area from two different and complementary points of view. The results from this study corroborate that the use of both radiotracers provides more useful comparative data than can be derived from the use of either tracer alone and therefore reinforce the coupled use of ^{238}U–^{234}Th and ^{210}Pb–^{210}Po disequilibria for a better understanding and more accurate determination of POC and total mass fluxes. This work also provides a basis to help plan future sampling strategies and promote further collaborative work in this field helping to reveal the more specific application of each tracer under specific oceanographic and biogeochemical conditions.

Acknowledgements

We are very grateful to Jim Murray for his input during the revision process. We would also like to thank Claudia Benitez-Nelson for her helpful comments, guidance and encouragement as well as the two other anonymous reviewers and the editor for their very useful remarks. EV has been supported by a Ph.D. Fellowship from Spain's Ministerio de Educación y Ciencia through Grant BES-2004-3348. We acknowledge funding to PM from Spain's Ministerio de Educación y Ciencia through Grant REN2002-10846-E/MAR. The MedFlux project was supported by the US National Science Foundation (Chemical Oceanography Programme). This is MSRC Contribution no. 1360 and MedFlux Contribution no. 20.

References

Armstrong, R.A., Lee, C., Hedges, J.I., Honjo, S., Wakeham, S.G., 2001. A new, mechanistic model for organic carbon fluxes in the ocean based on the quantitative association of POC with ballast minerals. Deep-Sea Research II 49, 219–236.

Bacon, M.P., Anderson, R.F., 1982. Distribution of thorium isotopes between dissolved and particulate forms in the deep sea. Journal of Geophysical Research 87, 2045–2056.

Bacon, M.P., Spencer, D.W., Brewer, P.G., 1976. Pb-210/Ra-226 and Po-210/Pb-210 disequilibria in seawater and suspended particulate matter. Earth and Planetary Science Letters 32, 277–296.

Bacon, M.P., Belastock, R.A., Tecotzky, M., Turekian, K.K., Spencer, D.W., 1988. Lead-210 and polonium-210 in ocean water profiles of the continental shelf and slope south of New England. Continental Shelf Research 8, 841–853.

Bacon, M.P., Cochran, J.K., Hirschberg, D.J., Hammar, T.R., Fleer, A.P., 1996. Export flux of carbon at the equator during the EqPac time-series cruises estimated from ^{234}Th measurements. Deep-Sea Research II 43, 1133–1153.

Benitez-Nelson, C., Buesseler, K.O., Rutgers van der Loeff, M., Andrews, J., Ball, L., Crossin, G., Charette, M., 2001. Testing a new small-volume technique for determining thorium-234 in seawater. Journal of Radioanalytical and Nuclear Chemistry 248 (3), 795–799.

Benitez-Nelson, C., Bidigare, R.R., Dickey, T.D., Landry, M.R., Leonard, C.L., Brown, S.L., Nencioli, F., Rii, Y.M., Maiti, K., Becker, J.W., Bibby, T.S., Black, W., Cai, W.J., Carlson, C., Chen, F.Z., Kuwahara, V.S., Mahaffey, C., McAndrew, P.M., Quay, P.D., Rappé, M., Selph, K.E., Simmons, M.E., Yang, E.J., 2007. Eddy induced diatom bloom drives increased biogenic silica flux, but inefficient carbon export in the subtropical North Pacific Ocean. Science 312, 1017–1021.

Benitez-Nelson, C.R., McGillicuddy, D.M., 2008. Mesoscale physical–biological–biogeochemical linkages in the open ocean: an introduction to the results of the E-Flux and EDDIES programs. Deep-Sea Research Part II, this issue [doi:10.1016/j.dsr2.2008.03.001].

Benitez-Nelson, C.R., Moore, W.S., 2006. Future applications of ^{234}Th in aquatic ecosystems. Marine Chemistry 100, 163–165.

Berelson, W.M., Johnson, K., Coale, K., Li, H.-C., 2002. Organic matter diagenesis in the sediments of the San Pedro Shelf along a transect affected by sewage effluent. Continental Shelf Research 22, 1101–1115.

Broecker, W.S., Li, Y.H., Cromwell, J., 1967. Radium-226 and radon-222: concentration in Atlantic and Pacific Oceans. Science 158, 1307–1310.

Brown, S.L., Landry, M.R., Selph, K.E., Yang, E.J., Rii, Y.M., Bidigare, R.R., 2008. Diatoms in the desert: plankton community response to a mesoscale eddy in the subtropical North Pacific. Deep-Sea Research II, this issue [doi:10.1016/j.dsr2.2008.02.012].

Buesseler, K.O., 1991. Do upper-ocean sediment traps provide an accurate record of particle flux? Nature 353, 420–423.

Buesseler, K.O., Bacon, M.P., Cochran, J.K., Livingstone, H.D., 1992. Carbon and nitrogen export during the JGOFS North Atlantic bloom experiment estimated from ^{234}Th:^{238}U disequilibria. Deep-Sea Research 39, 1115–1137.

Buesseler, K.O., Andrews, J.A., Hartman, M.C., Belastock, R., Chai, F., 1995. Regional estimates of the export flux of particulate organic carbon derived from thorium-234 during the JGOFS EqPac program. Deep-Sea Research I 42, 777–804.

Buesseler, K.O., Steinberg, D.K., Michaels, A.F., Johnson, R.J., Andrews, J.E., Valdes, J.R., Price, J.F., 2000. A comparison of the quantity and quality of material caught in a neutrally buoyant versus surface-tethered sediment trap. Deep-Sea Research. Part 1. Oceanographic Research Papers 47, 277–294.

Buesseler, K.O., Benitez-Nelson, C., Rutgers van der Loeff, M., Andrews, J., Ball, L., Crossin, G., Charette, M., 2001. An intercomparison of small- and large-volume techniques for thorium-234 in seawater. Marine Chemistry 74 (1), 15–28.

Buesseler, K.O., Benitez-Nelson, C.R., Moran, S.B., Burd, A., Charette, M., Cochran, J.K., Coppola, L., Fisher, N.S., Fowler, S.W., Gardner, W.D., Guo, L.D., Gustafsson, Ö., Lamborg, C., Masque, P., Miquel, J.C., Passow, U., Santschi, P.H., Savoye, N., Stewart, G., Trull, T., 2006. An assessment of particulate organic carbon to thorium-234 ratios in the ocean and their impact on the application of ^{234}Th as a POC flux proxy. Marine Chemistry 100, 213–233.

Buesseler, K.O., Antia, A.N., Chen, M., Fowler, S.W., Gardner, W.D., Gustafsson, O., Harada, K., Michaels, A.F., Rutgers van der Loeff, M., Sarin, M., Steinberg, D.K., Trull, T., 2007. An assessment of the use of sediment traps for estimating upper ocean particle fluxes. Journal of Marine Research 65, 345–416.

Buesseler, K.O., Lamborg, C., Cai, P., Escoube, R., Johnson, R., Pike, S., Masqué, P., McGillicuddy, D., E. Verdeny, E., 2008. Particle fluxes associated with mesoscale eddies in the Sargasso Sea. Deep-Sea Research Part II, this issue [doi:10.1016/j.dsr2.2008.02.007].

Chai, F., Lindley, S.T., Barber, R.T., 1995. Origin and maintenance of a high nitrate condition in the equatorial Pacific. A biological–physical model study. Ph.D. Thesis, Duke University, 170pp.

Charette, M.A., Moran, S.B., 1999. Rates of particle scavenging and particulate organic carbon export estimated using ^{234}Th as a tracer in the subtropical and equatorial Atlantic Ocean. Deep-sea Research II 46, 885–906.

Chen, J.H., Edwards, G.J., Wasserburg, G.J., 1986. ^{238}U, ^{234}Th and ^{232}Th in sea water. Earth and Planetary Science Letters 80, 241–251.

Cherrier, J., Burnett, W.C., LaRock, P.A., 1995. Uptake of polonium and sulfur by bacteria. Geomicrobiology Journal 13, 103–115.

Coale, K.H., Bruland, K.W., 1985. ^{234}Th:^{238}U disequilibria within the California Current. Limnology and Oceanography 30, 22–33.

Cochran, J.K., 1992. The oceanic chemistry of the uranium and thorium series nuclides. Uranium series disequilibrium: applications to earth, marine and environmental sciences. M. Ivanovich, OUP, 334–395.

Cochran, J.K., Masqué, P., 2003. Short-lived U/Th Series radoionuclides in the ocean: tracers for scavenging rates, export fluxes and particle dynamics. Reviews in Mineralogy & Geochemistry 52, 461–492.

Cochran, J.K., Hirschberg, D.J., Livingston, H.D., Buesseler, K.O., Key, R.M., 1995. Natural and anthropogenic radionuclide distributions in the Nansen Basin, Arctic Ocean: scavenging rates and circulation timescales. Deep-Sea Research Part II 42 (6), 1495–1517.

Cochran, J.K., Miquel, J-C., Armstrong, R., Fowler, S., Masqué, P., Gasser, B., Hirschberg, D., Szlosek, J., Rodriguez y Baena, A.M., Verdeny, E., Stewart, G., 2009. Time-series measurements of ^{234}Th in water column and sediment trap samples from the northwestern Mediterranean. Deep-Sea Research Part II, this issue [doi:10.1016/j.dsr2.2008.12.034].

Dickey, T., Nencioli, F., Kuwahara, V., Leonard, C., Black, W., Bidigare, R., Rii, Y., Zhang, Q., 2008. Physical and bio-optical observations of oceanic cyclones west of the island of Hawaii. Deep-Sea Research Part II, this issue [doi:10.1016/j.dsr2.2008.01.006].

Ducklow, H.D., Steinberg, D.K., Buesseler, K.O., 2001. Upper ocean carbon export and the biological pump. Oceanography 14 (4), 50–58.

Eppley, R.W., Peterson, B.J., 1979. Particulate organic matter flux and planktonic new production in the deep ocean. Nature 282, 677–680.

Feely, R.A., Sabine, C.L., Takahashi, T., Wanninkhof, R., 2001. Uptake and storage of carbon dioxide in the oceans: the global CO_2 survey. Oceanography 14 (4), 18–32.

Fisher, N.S., Burns, K.A., Cherry, R.D., Heyraud, M., 1983. Accumulation and cellular distribution of ^{241}Am, ^{210}Po and ^{210}Pb in two marine algae. Marine Ecology Progress Series 11, 233–237.

Friedrich, J., Rutgers van der Loeff, M.M., 2002. A two-tracer (^{210}Po–^{234}Th) approach to distinguish organic carbon and biogenic silica export flux in the Antarctic circumpolar current. Deep-Sea Research I 49, 101–120.

Gardner, W.D., 1980. Sediment trap dynamics and calibration: a laboratory evaluation. Journal of Marine Research 38, 17–39.

Gardner, W.D., 2000. Sediment trap technology and surface sampling in surface waters. In: Hanson, R.B., Ducklow, H.W., Field, J.G. (Eds.), The Changing Ocean Carbon Cycle, a Midterm Synthesis of the Joint Global Ocean Flux Study. Cambridge University Press, Cambridge, pp. 240–281.

Gust, G., Byrne, R.H., Bernstein, R.E., Betzer, P.R., Bowles, W., 1992. Particle fluxes and moving fluids: experience from synchronous trap collections in the Sargasso Sea. Deep-Sea Research 39, 1071–1983.

Gust, G., Michaels, A.F., Jonson, R., Dueser, W.D., Barber, W., 1994. Mooring line motions and sediment trap hydrodynamics: *in situ* intercomparison of three common deployment designs. Deep-Sea Research I 41, 831–858.

Heyraud, M., Fowler, S.W., Beasley, T.M., Cherry, R.D., 1976. Polonium-210 in euphausiids: a detailed study. Marine Biology 34, 127–138.

Honeyman, B.D., Balistrieri, L.S., Murray, J.W., 1988. Oceanic trace metal scavenging: the importance of particle concentration. Deep-Sea Research 35, 227–246.

Honjo, S., Manganini, S.J., Cole, J.J., 1982. Sedimentation of biogenic matter in the deep ocean. Deep-Sea Research 29, 608–625.

Honjo, S., Dymond, J., Collier, R., Manganini, S.J., 1995. Export production of particles to the interior of the equatorial Pacific Ocean during the 1992 EqPac experiment. Deep-Sea Research II 42, 831–870.

Honjo, S., Francois, R., Manganini, S., Dymond, J., Collier, R., 2000. Particle fluxes to the interior of the Southern Ocean in the Western Pacific sector along 170°W. Deep-Sea Research II 47, 3521–3548.

Karl, D.M., Knauer, G.A., 1989. Swimmers: a recapitulation of the problem and a potential solution. Oceanography 2, 32–35.

Kharkar, D.P., Thomson, J., Turekian, K.K., Forster, W.O., 1976. Uranium and thorium decay series nuclides in plankton from the Caribbean. Limnology and Oceanography 21, 294–299.

Kim, G., Church, T.M., 2001. Seasonal biogeochemical fluxes of ^{234}Th and ^{210}Po in the upper Sargasso Sea: influence from atmospheric iron deposition. Global Biogeochemical Cycles 15, 651–661.

Knauer, G.A., Redalje, D.G., Harrison, W.G., Karl, D.M., 1990. New production at the VERTEX time-series site. Deep-Sea Research 37, 1121–11134.

Kritz, M.A., 1983. Use of long-lived Radon daughters as indicators of exchange between the free troposphere and the marine boundary layer. Journal of Geophysical Research 88, 8569–8573.

Ku, T.-L., Li, Y.H., Mathieu, G.G., Wong, H.K., 1970. Radium in the Indian-Antarctic Ocean south of Australia. Journal of Geophysical Research 75, 5286–5292.

Ku, T.-L., Lin, M.C., 1976. Ra-226 distributions in the Antarctic Ocean. Earth Planetary Science Letters 31, 236–248.

Kuwahara, V.S., Nencioli, F., Dickey, T.D., Rii, Y.M., Bidigare, R.R., 2008. Physical dynamics and biological implications of cyclonic eddy *Noah* in the lee of Hawaii during E-Flux I. Deep-Sea Research Part II, this issue [doi:10.1016/j.dsr2.2008.01.007].

Lambert, G., Polian, G., Sanak, J., Ardouin, B., Buisson, A., Jegu, A., Le Roulley, J.C., 1982. Cycle du radon et des ces descendents: application a l'etude des changes troposphere stratosphere. Annales Geophysicae 38, 497–531.

Landry, M.R., Decima, M., Simmons, M.P., Hannides, C.C.S., Daniels, E., 2008. Mesozooplankton biomass and grazing responses to Cyclone Opal, a subtropical mesoscale eddy. Deep-Sea Research II, this issue [doi:10.1016/j.dsr2.2008.01.005].

Langmuir, D., 1978. Uranium solution-mineral equilibria at low-temperatures with applications to sedimentary ore-deposits. Geochimica et Cosmochimica Acta 42 (6), 547–569.

Lee, C., Wakeham, S.G., Hedges, J.I., 1988. The measurement of oceanic particle flux—are "swimmers" a problem? Oceanography 1, 34–36.

Liu, Z., Stewart, G., Cochran, J.K., Lee, C., Armstrong, R.A., Hirschberg, D.J., Gasser, B., Miquel, J.-C., 2005. Why do POC concentrations measured using Niskin bottle collections differ from those using in situ pumps? Deep-Sea Research. Part 1. Oceanographic Research Papers 52, 1324–1344.

Maiti, K., Benitez-Nelson, C., Rii, Y.M., Bidigare, R.R., 2008. Influence of a mature cyclonic eddy on particle export in the lee of Hawaii. Deep-Sea Research Part II, this issue [doi:10.1016/j.dsr2.2008.02.008].

Martin, J.H., Knauer, G.A., Karl, D.M., Broenkow, W.W., 1987. VERTEX: carbon cycling in the northeast Pacific. Deep-Sea Research II 34, 267–285.

Masqué, P., Sanchez-Cabeza, J.A., Bruach, J.M., Palacios, E., Canals, M., 2002. Balance and residence times of ^{210}Pb and ^{210}Po in surface waters of the northwestern Mediterranean Sea. Continental Shelf Research 22, 2127–2146.

Matsumoto, E., 1975. ^{234}Th–^{238}U radioactive disequilibrium in the surface layer of the ocean. Geochimica et Cosmochimica Acta 39, 205–212.

Michaels, A.F., Silver, M.W., Gowing, M.M., Knauer, G.A., 1990. Cryptic zooplankton "swimmers" in upper ocean sediment traps. Deep-Sea Research 37, 1285–1296.

Moore, R.M., Hunter, K.A., 1985. Thorium adsorption in the ocean: reversibility and distribution amongst particle sizes. Geochimica et Cosmochimica Acta 49, 2253–2257.

Moore, H.E., Poet, S.E., Martell, E.A., Wilkening, L.H., 1974. Origin of Rn-222 and its long-lived daughters in air over Hawaii. Journal of Geophysical Research 79, 5019–5024.

Moran, S.B., Ellis, K.M., Smith, J.N., 1997. ^{234}Th/^{238}U disequilibrium in the central Arctic Ocean: implications for particulate organic carbon export. Deep-Sea Research II 44, 1593–1606.

Moran, S.B., Charette, M.A., Pike, S.M., Wicklund, C.A., 1999. Differences in seawater particulate organic carbon concentration in samples collected using small-volume and large-volume methods: the importance of DOC adsorption to the filter blank. Marine Chemistry 67, 33–42.

Murray, J.W., Young, J., Newton, J., Dunne, J., Chapin, T., Paul, B., McCarthys, J.J., 1996. Export flux of particulate organic carbon from the Central Equatorial Pacific determined using a combined drifting trap-^{234}Th approach. Deep-Sea Research II 43, 1095–1132.

Murray, J.W., Paul, B., Dunne, J.P., Chapin, T., 2005. ^{234}Th, ^{210}Pb, ^{210}Po and stable Pb in the Central Equatorial Pacific: tracers for particle cycling. Deep-Sea Research I 52, 2109–2139.

Nencioli, F., Dickey, T.D., Kuwahara, V.S., Black, W., Rii, Y.M., Bidigare, R.R., 2008. Physical dynamics and biological implications of a mesoscale cyclonic eddy in the lee of Hawaii: cyclone *Opal* observations during E-Flux III. Deep-Sea Research Part II, this issue [doi:10.1016/j.dsr2.2008.02.003].

Nozaki, J., Turekian, K.K., 1976. Ra-226, Pb-210 abd Po-210 diesquilibria in the western North-Pacific. Earth and Planetary Science Letters 32 (2), 313–321.

Nozaki, Y., Thomson, J., Turekian, K.K., 1976. The distributions of Pb-210 and Po-210 in the surface waters of the Pacific Ocean. Earth and Planetary Science Letters 32, 304–312.

Pates, J.M., Muir, G.K.P., 2007. U–salinity relationships in the Mediterranean: implications for ^{234}Th:^{238}U particle flux studies. Marine Chemistry 106 (3–4), 530–545.

Peterson, M.L., Wakeham, S.G., Lee, C., Askea, M., Miquel, J.C., 2005. Novel techniques for collection of sinking particles in the ocean and determining their settling rates. Limnology and Oceanography: Methods 3, 520–532.

Rutgers van der Loeff, M.M., Friedrich, J., Bathmann, U.V., 1997. Carbon export during the Spring Bloom at the Antarctic Polar Front, determined with the natural tracer ^{234}Th. Deep-Sea Research II 44, 457–478.

Santschi, P.H., Murray, J.W., Baskaran, M., Benitez-Nelson, C.R., Guo, L., Hung, C.-C., Lamborg, C., Moran, S.B., Passow, U., Roy-Barman, M., 2006. Thorium speciation in seawater. Marine Chemistry 100, 250–268.

Sarin, M.M., Guebuem, K., Church, T.M., 1999. ^{210}Po and ^{210}Pb in the South-equatorial Atlantic: distribution and disequilibrium in the upper 500 m. Deep-Sea Research II 46, 907–917.

Savoye, N., Benitez-Nelson, C., Burd, A.B., Cochran, J.K., Charette, M., Buesseler, K.O., Jackson, G., Roy-Barman, M., Schmidt, S., Elskens, M., 2006. ^{234}Th sorption and export models in the water column: a review. Marine Chemistry 100, 234–249.

Shannon, L.V., Cherry, R.D., Orren, M.J., 1970. Polonium-210 and lead-210 in the marine environment. Geochimica et Cosmochimica Acta 34, 701–711.

Shimmield, G.B., Ritchie, G.D., Fileman, T.W., 1995. The impact of marginal ice zone processes on the distribution of ^{210}Pb, ^{210}Pb and ^{234}Th and implications for new production in the Bellingshausen Sea. Antarctica Deep-Sea Research II 42, 1313–1335.

Steinberg, D.K., Carlson, C.A., Bates, N.R., Johnson, R.J., Michaels, A.F., Knap, A.H., 2001. Overview of the JGOFS Bermuda Atlantic time-series study (BATS): a decade-scale look at ocean biology and biogeochemistry. Deep-Sea Research II 48, 1405–1447.

Stewart, G.M., Fisher, N.S., 2003a. Experimental studies on the accumulation of polonium-210 by marine phytoplankton. Limnology and Oceanography 48 (3), 1193–1201.

Stewart, G.M., Fisher, N.S., 2003b. Bioaccumulation of polonium-210 in marine copepods. Limnology and Oceanography 48 (5), 2011–2019.

Stewart, G.M., Fowler, S.W., Teyssie, J.-L., Cotret, O., Cochran, J.K., Fisher, N.S., 2005. Contrasting the transfer of polonium-210 and lead-210 across three trophic levels in the marine plankton. Marine Ecology Progress Series 290, 27–33.

Stewart, G., Cochran, J.K., Xue, J., Lee, C., Wakeham, S.G., Armstrong, R.A., Masque, P., 2007a. Exploring the connection between ^{210}Po and organic matter in the northwestern Mediterranean. Deep-Sea Research I 54, 415–427.

Stewart, G., Cochran, J.K., Miquel, J.C., Masqué, P., Szlosek, J., Rodriguez y Baena, A.M., Fowler, S.W., Gasser, B., Hirschberg, D.J., 2007b. Comparing POC export from ^{234}Th/^{238}U and ^{210}Po/^{210}Pb disequilibria with estimates from sediment traps in the northwest Mediterranean. Deep-Sea Research I 54, 1549–1570.

Turekian, K.K., Kharkhar, D.P., Thomson, J., 1974. The fates of ^{210}Pb and ^{210}Po in the ocean surface. Journal Rechargeable Atmosphere 8, 639–646.

Turekian, K.K., Nozaki, Y., Benninger, L.K., 1977. Geochemistry of atmospheric radon and radon products. Annual Review of Earth and Planetary Science 5, 227–255.

Verdeny, E., Masque, P., Maiti, K., Garcia-Orellana, J., Bruach, J.M., Benitez-Nelson, C.R., 2008. Particle export within cyclonic Hawaiian lee eddies derived from ^{210}Pb–^{210}Po disequilibria. Deep-Sea Research Part II, this issue [doi:10.1016/j.dsr2.2008.02.009].